



Listen to your heart: Trade-off between cardiac interoceptive processing and visual exteroceptive processing

Qiaoyue Ren, Amanda C. Marshall, Junhui Liu, Simone Schütz-Bosbach*

Department of Psychology, General and Experimental Psychology Unit, LMU Munich, Leopoldstr. 13, Munich 80802, Germany

ARTICLE INFO

Keywords:

Cardiac signals
Cardiac systole
Cardiac diastole
EEG
Heartbeat-evoked potential
Steady-state visual evoked potential

ABSTRACT

Internal bodily signals, such as heartbeats, can influence conscious perception of external sensory information. Spontaneous shifts of attention between interoception and exteroception have been proposed as the underlying mechanism, but direct evidence is lacking. Here, we used steady-state visual evoked potential (SSVEP) frequency tagging to independently measure the neural processing of visual stimuli that were concurrently presented but varied in heartbeat coupling in healthy participants. Although heartbeat coupling was irrelevant to participants' task of detecting brief color changes, we found decreased SSVEPs for systole-coupled stimuli and increased SSVEPs for diastole-coupled stimuli, compared to non-coupled stimuli. These results suggest that attentional and representational resources allocated to visual stimuli vary according to fluctuations in cardiac-related signals across the cardiac cycle, reflecting spontaneous and immediate competition between cardiac-related signals and visual events. Furthermore, frequent coupling of visual stimuli with stronger cardiac-related signals not only led to a larger heartbeat evoked potential (HEP) but also resulted in a smaller color change evoked N2 component, with the increase in HEP amplitude associated with a decrease in N2 amplitude. These findings indicate an overall or longer-term increase in brain resources allocated to the internal domain at the expense of reduced resources available for the external domain. Our study highlights the dynamic reallocation of limited processing resources across the internal-external axis and supports the trade-off between interoception and exteroception.

1. Introduction

Our brain receives signals from both the external environment and inside our body. Internal bodily processes, such as heartbeats, can influence our processing of external information (Tallon-Baudry, 2023). In a single heartbeat or cardiac cycle, there are two main cardiac phases: during systole, the heart ejects the blood, whereas during diastole, it refills (DeSaix et al., 2013). Therefore, cardiac-related physiological signals naturally fluctuate throughout the cardiac cycle. The perception of external stimuli is typically reduced during the cardiac phase considered to have strong versus weak cardiac-related signals, although the temporal definition of cardiac phase/timing with strong or weak cardiac-related signals varies across studies (Al et al., 2020; Edwards et al., 2008; Ren et al., 2022a; but see Elliott and Graf, 1972 for null effect and Garfinkel et al., 2014 for opposite effect). For instance, in some studies presenting exteroceptive stimuli at specific timings after the onset of cardiac cycle (indicated by R-peak in the electrocardiogram; ECG), researchers observed reduced exteroception during the middle phase (approximately 200–500 ms after the R-peak) of cardiac cycle,

compared to the earlier (approximately 0–150 ms after the R-peak) and/or later phases (approximately 600–750 ms after the R-peak; Edwards et al., 2008; 2007; 2001; Ren et al., 2022a). These studies defined the middle phase as the "systole" phase during which strong cardiac-related signals are assumed to be sent to the brain, and the remaining period as the "diastole" phase with weak cardiac-related inputs. Some other studies, which presented exteroceptive stimuli randomly and determined their position in the cardiac cycle a posteriori, observed reduced perceptual sensitivity and responses to stimuli occurring between ECG R-peak and the end of T-wave (defined as the "systole" phase with strong cardiac-related signals) compared to the remaining period or an equivalent length at the end of the cardiac cycle (defined as the "diastole" phase with weak cardiac-related signals; Al et al., 2021, 2020; Grund et al., 2022). These cardiac cycle effects on perception have been explained by an attentional trade-off framework, which posits that attentional resources are shared and competed for between interoception and exteroception (Al et al., 2020; Bernston and Khalsa, 2021; Critchley and Garfinkel, 2018; Galvez-Pol et al., 2020, 2022b; Khalsa et al., 2018; Ren et al., 2022a). Specifically, increased

* Corresponding author.

E-mail address: S.Schuetz-Bosbach@psy.lmu.de (S. Schütz-Bosbach).

<https://doi.org/10.1016/j.neuroimage.2024.120808>

Received 2 April 2024; Received in revised form 21 August 2024; Accepted 22 August 2024

Available online 23 August 2024

1053-8119/© 2024 The Authors. Published by Elsevier Inc. This is an open access article under the CC BY license (<http://creativecommons.org/licenses/by/4.0/>).

attentional resources directed to the internal domain lead to reduced resources available for the external domain, thereby diminishing the perception of external stimuli.

Our study aimed to provide further evidence for this trade-off pattern between interoceptive and exteroceptive processing. First, most previous studies examined the cardiac cycle effect on the perception of single, transient sensory stimulation (e.g., Al et al., 2020; Edwards et al., 2007; Grund et al., 2022), leaving an unanswered question—whether the attention allocated to multiple, continuous sensory stimuli differs when some are coupled to strong cardiac-related signals and the others to weaker cardiac-related signals. Second, prior research primarily focused on how responses to external sensory stimuli vary according to the estimated changes in cardiac-related signals (e.g., Edwards et al., 2008, 2001; Pramme et al., 2016, 2014), without directly measuring the cardiac-related signals or processes at the specific timing or phase when the external events occurred. To better explore the trade-off between cardiac and visual processing, it is more effective to directly test whether increases in cardiac processing correspond to decreases in visual processing during the same period. Some researchers have explored the relationship between pre-stimulus heartbeat evoked potential (HEP) and the subsequent sensory evoked potential (Al et al., 2020; Marshall et al., 2020; Park et al., 2014). However, this relationship reflects how changes in pre-stimulus interoception modulate subsequent exteroception, rather than simultaneous changes in interoception and exteroception. Third, existing evidence for the cardiac cycle effect on exteroception only suggests that the allocation of attentional resources to external sensory information varies according to the fluctuations of cardiac-related signals in each cardiac cycle. It remains unclear whether the co-occurrence of strong cardiac-related signals with visual information results in a general or longer-term regulation in the relative proportion of attention allocated to the internal and external domains.

To address these issues, we employed a dynamic visual detection task with simultaneous electrocardiogram (ECG) and electroencephalogram (EEG) recordings. Participants observed two groups of moving dots that differed in color, flickering frequency, and motion direction. One group changed direction at random times within each cardiac cycle (non-coupled dots), while the other group changed direction during either strong cardiac-related signals (systole-coupled dots), weak cardiac-related signals (diastole-coupled dots), or randomly within each cardiac cycle (non-coupled dots). Notably, the direction changes of the non-coupled dots sometimes coincided with strong cardiac-related signals at systole and sometimes with weak cardiac-related signals at diastole within one trial, resulting in an average alignment with medium-level cardiac-related signals, i.e., lower than the systole-coupled dots but higher than the diastole-coupled dots. Participants' task was to detect a brief color change occurring at a random time during the presentation of the dots, primarily to maintain their engagement throughout the task. The heartbeat coupling of the direction changes was irrelevant to their task goal, allowing us to explore the spontaneous shifts of processing resources along the internal-external axis. This complements earlier studies focusing on intentional shifts between interoception and exteroception (Kritzman et al., 2022; Petzschner et al., 2019; Villena-González et al., 2017).

Importantly, as the two groups of dots flickered at different frequencies, we could independently measure the brain responses to each group using steady-state visual evoked potential (SSVEP) frequency tagging. SSVEPs are continuous neurophysiological responses elicited by a visual stimulus with periodic luminance or contrast modulation, producing oscillatory activity at the driving frequency as well as its higher harmonics (Norcia et al., 2015). By comparing the SSVEPs evoked by the dots with direction changes coupled with strong or weak cardiac-related signals versus those coinciding with medium-level cardiac-related signals, we could explore whether different levels of attention were selectively allocated to the two groups of dots presented concurrently in the same visual field but disturbed by different strengths of cardiac-related signals.

According to the attentional trade-off theory, we expected reduced visual representations of direction changes when cardiac-related signals are strong, compared to when these signals are weaker. Given that SSVEPs capture the cumulative brain responses to visual events associated with the flickering dots, and all visual events in both groups of dots, except for the heartbeat coupling of direction changes, were identical or counterbalanced, we hypothesized that systole-coupled dots would trigger lower SSVEPs, while diastole-coupled dots would trigger larger SSVEPs, compared to concurrently-presented non-coupled dots.

We also analyzed participants' HEP while they observed the moving dots and the visual evoked potential (VEP) evoked by the color change. The HEP reflects cardiac processing in the brain (Coll et al., 2021; Park et al., 2018) and is modulated by attention directed toward cardiac system (Kritzman et al., 2022; Petzschner et al., 2019). The VEP, specifically the N2 component, is regarded as an indicator of visual sensitivity and awareness (Eiserbeck et al., 2022; Koivisto and Grassini, 2016).

By separately comparing HEP amplitude and VEP amplitude across the three conditions, we could explore the longer-term effects of heartbeat coupling on the regulation of brain resources allocated to internal and external domain, respectively. We hypothesized that the co-occurrence of direction changes with stronger cardiac-related signals would result in an overall increase in the brain's attention to internal cardiac system (manifested as increased HEP amplitude) and simultaneously lead to a general decrease in attentional resources available for external events (e.g., color change) in the continuous visual stimuli (manifested as decreased VEP amplitude and a potential decreased color detection performance). Moreover, we expected the increase in cardiac processing to be associated with a decrease in the processing of the color change, indicating a trade-off between brain resources allocated to interoception and exteroception.

2. Materials and methods

2.1. Participants

Thirty-two participants (20 females; age: 25.69 ± 6.28 years [mean \pm SD], range: 19–44 years) were recruited from the university participant database. To the best of our knowledge, no previous studies had explored the cardiac cycle effect on SSVEPs in a similar task. Therefore, we could not compute the required sample size a priori. However, our sample size is comparable with relevant previous studies (Gjorgieva et al., 2022; Kritzman et al., 2022; Ren et al., 2022a). Furthermore, a post-hoc power analysis, conducted using the MorePower software (Campbell and Thompson, 2012), indicates that our sample size is sufficient for detecting effects with an η_p^2 of 0.14 in a one-way (3 levels) repeated measures ANOVA, as well as effects with an η_p^2 of 0.21 in a three-way ($2 \times 2 \times 2$) repeated measures ANOVA, both with a power of 0.80 and α of 0.05. All the participants reported normal or corrected-to-normal visual acuity, no color blindness, no diagnosed heart-rhythm abnormalities, no present or past psychiatric or neurological disorders, and no current use of medication. The study was approved by the local ethics committee at the Department of Psychology of LMU Munich in accordance with the Declaration of Helsinki. All participants provided written informed consent and received either financial compensation (9 euros per hour) or course credit for their participation.

2.2. Experimental design

In the dynamic visual detection task (see Fig. 1A), participants were required to detect a brief color change in the dots' frame while observing two groups of moving dots that differed in color, flickering frequency, and motion direction. This color change detection task primarily served to maintain participants' engagement. The key experimental manipulation involved coupling the timing of the direction changes with

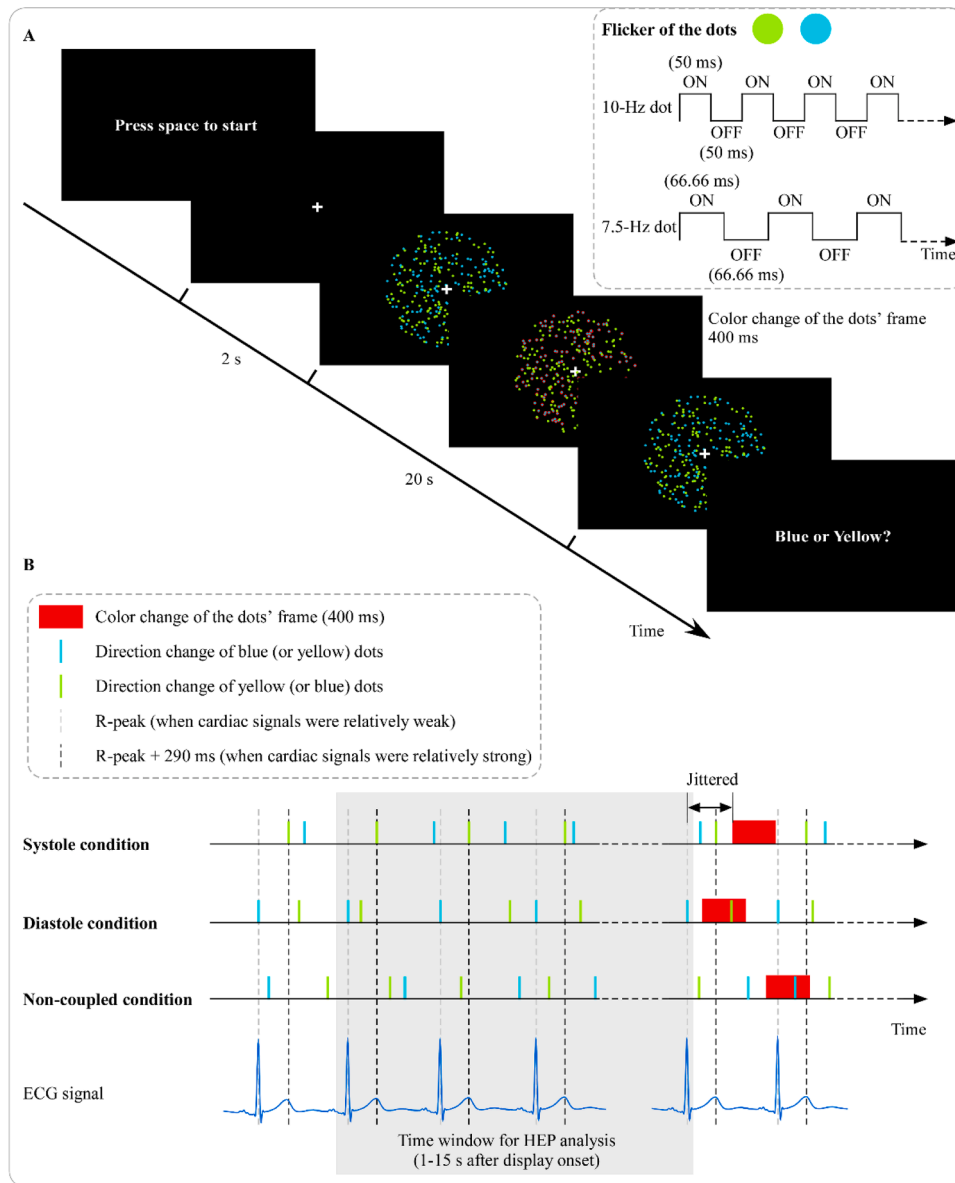


Fig. 1. The dynamic visual detection task. (A) Timeline of each trial. Participants observed two groups of random dots that differed in color, flickering frequency, and motion direction, and then reported the color of the dots whose frame had briefly flashed to red. **(B)** Experimental conditions. Systole condition: one group of colored dots always changed direction when cardiac-related signals were strong, while the other group changed direction at a random time within each cardiac cycle (i.e., coinciding with on average medium-level cardiac-related signals). Diastole condition: one group of colored dots always changed direction when cardiac-related signals were weak, while the other group changed direction at a random time within each cardiac cycle. Non-coupled condition: both groups of colored dots changed direction at random times within each cardiac cycle.

different cardiac phases (see Fig. 1B).

The experiment included three trial types.

In Systole trials, the direction change of one group of colored dots (blue or yellow) was designed to always occur at 290 ms after the R-peak, to coincide with the end of ventricular systole, i.e., when cardiac-related signals were relatively strong (Marshall et al., 2022; Rae et al., 2018; Ren et al., 2022b). The direction change of the other group of colored dots occurred at a random time within 0–600 ms after the R-peak, to be out of sync with cardiac cycle. This condition was designed to compare the SSVEPs of the systole-coupled versus non-coupled dots.

In Diastole trials, the direction change of one group of colored dots was designed to always occur at the R-peak, to coincide with the end of ventricular diastole, i.e., when cardiac-related signals were relatively low (DeSaix et al., 2013; Garfinkel et al., 2014; Ren et al., 2022a). The direction change of the other group of colored dots occurred at a random time within 0–600 ms after the R-peak. This condition was designed to

compare the SSVEPs of the diastole-coupled versus non-coupled dots.

In Non-coupled trials, the direction changes of both groups of colored dots occurred at random times within 0–600 ms after the R-peak, serving as the control condition.

The brief color change occurred only once per trial and at a random time during the presentation of the dots. It is not coupled to any specific cardiac phase.

2.3. Stimuli and procedure

Participants were seated in a dimly lit room at 70 cm from a monitor (24 inches; refresh rate: 60 Hz; resolution: 1920 × 1080 pixels) with their heads on a chin rest. The visual displays were generated and displayed using the Presentation software (Neurobehavioral Systems, Inc.).

Each visual display consisted of 300 blue (luminance: 203 cd/m²) and yellow (203 cd/m²) dots (150 of each; diameter: 0.23° of visual

angle). These dots were randomly distributed within an invisible circle (radius: 5.00°) at the center of the screen that was marked with a white (245 cd/m^2) fixation cross. The background was black (0.3 cd/m^2). The dots were drawn in a random order to prevent depth perception and were continuously in motion, moving at a velocity of 0.08° . Dots that moved out of the invisible circle immediately disappeared but reappeared on the opposite side of the circle. Specifically, their location shifted from $[x, y]$ to $[-x, -y]$, given that the center of the screen was located at $[0, 0]$. Therefore, participants always saw 300 dots. The motion of the dots in the same color was the same, but differed from the dots of the other color. Participants were therefore able to perceive two distinct groups of moving dots using color and coherent movements. The two groups of dots changed their motion direction dynamically (deviated randomly by plus $60\text{--}300^\circ$ from the original direction) while keeping their directions different at any time (the absolute difference between the two directions was always greater than 60°).

The two groups of dots flickered at different frequencies, either 7.5 or 10 Hz, with a 50/50 on/off duty cycle. We selected these frequencies based on the following criteria: 1) Stimulus frequencies in SSVEP studies typically range from 3 to 20 Hz (Norcía et al., 2015); 2) The available frequencies for tagging on a 60 Hz monitor are derived from dividing 60 Hz by integers (e.g., $60/6$); 3) The frequencies should not exhibit harmonic relationships, where one frequency is an integer multiple of another (e.g., 6 and 12 Hz; Figueira et al., 2022); 4) The frequencies should be close enough to prevent the two groups of dots from appearing significantly different. Although the two groups of dots might partially and briefly overlap during motion, they remained visible due to their distinct flickering frequencies.

As depicted in Fig. 1A, participants pressed the space key on the keyboard to start each trial when they felt ready. After 2 s, a dynamic visual display appeared, lasting for 20 s. Participants were instructed to pay equal attention to both groups of dots, and to detect a brief (400 ms) red flashing frame (frame width: 0.02° ; luminance: 60 cd/m^2) on one group of colored dots. The red frame flickered at the same frequency as the dots. Participants were instructed to continue observing the visual display until it disappeared, even after having seen the color change. Participants then pressed either the "F" key for blue dots or the "J" key for yellow dots to indicate which group of dots' frame briefly flashed to red during the trial. They were not given any feedback about their response. After their response, a blank screen was displayed on the screen for 1.5 s, followed by the start screen of the next trial. Participants were instructed to keep their gaze fixed on the central cross throughout the trial and to avoid intentionally focusing on a specific or partial area of the moving dots or actively shifting their gaze between different parts of the visual stimuli.

The color change of the dots' frame and the experience of having already detected it (successfully finding the target) can potentially influence participants' attention towards the dots during the remaining time of the trial, which may interfere with the anticipated effect of heartbeat coupling on SSVEPs. Therefore, in a majority of trials, the color change was designed to appear at the end of each trial (> 15 s after display onset), and the data of the last 5 s in these trials were excluded for SSVEP analysis (see Section 2.5.3.1). In addition, if the color change always appeared at the end of each trial, participants might have become aware of this pattern at the cost of paying full attention at the very beginning of each trial. Therefore, we also added few trials presenting the color change early (< 15 s after display onset), while these trials were excluded for SSVEP analysis. Specifically, the color change occurred between 5 and 10 s after display onset with a probability of $1/12$, between 10 and 15 s with a probability of $1/12$, between 15 and 17 s with a probability of $5/12$, and between 17 and 19 s with a probability of $5/12$.

To get familiar with the experimental procedure, participants completed a practice session consisting of three trials (one trial for each trial type in a random order), with accuracy feedback provided. The experiment comprised 5 blocks, with 24 trials per block. Each block

included 10 Systole trials, 10 Diastole trials, and 4 Non-coupled trials, presented in a random order. Participants took self-paced breaks between blocks. Additionally, a resting block (duration: 2.5 min) was conducted before the visual detection task, during which participants were asked to focus on the centrally presented fixation cross with no other visual stimuli. The study lasted approximately 1 h, preceded by about 1 h of preparation.

2.4. Data acquisition

For EEG recording, we used 65 active electrodes (BrainProducts ActiSnap) and one additional ground electrode positioned following the international 10–20 system. The FCz functioned as the online reference for these scalp electrodes. For ECG recording, we used 3 electrodes placed below the left clavicle (reference electrode), the right clavicle (ground electrode), and the left pectoral muscle (active electrode). All electrophysiological signals were recorded with a 1000 Hz sampling rate and a 0.1–1000 Hz online bandpass filter. All impedances were kept below 20 k Ω . The BrainVision Recorder software (Brain Products, Inc.) was used for signal acquisition and amplification. The BrainVision RecView software (Brain Products, Inc.) was employed to achieve online detection of ECG R-peaks. R-peaks were identified as the first sample of decreasing voltage after surpassing a predetermined threshold. The threshold for detecting R-peaks was individually set by the experimenter after visually examining the 2.5 min ECG signal during the resting block. Each time an R-peak was detected, a pulse was sent to the experimental PC.

2.5. Data quantification

2.5.1. EEG and ECG pre-processing

EEG pre-processing was performed using the FieldTrip toolbox (Oostenveld et al., 2011) in Matlab (Mathworks Inc., Natick, MA; version R2019b). The EEG data were re-referenced to the average of the left and right-mastoids, filtered using a 60 Hz low-pass filter, and segmented into epochs ranging from -2 to 20 s relative to the onset of the visual display. No bad electrodes were found during the analysis. Independent component analysis was employed, and the stereotypical components reflecting eye movements and blinks were manually identified and removed based on scalp topography and time course. On average, 2.22 ± 1.04 components per participant were removed, and artifact-free EEG data were obtained by back-projecting the remaining components onto the scalp electrodes.

2.5.2. Stimulus timing and heartbeat coupling

A post hoc analysis was performed to check the precision of the R-peak detection and the intervals between the R-peaks and the direction changes of the dots throughout the experiment. Specifically, we used *findpeaks* function in Matlab to identify the timings of the R-peaks in the offline ECG data in each trial, and then compared them with the timings of the direction changes of each group of dots. Trials with imprecise R-peak detection (hit rate < 0.80 or false alarm rate > 0.20 ; 4.75 ± 7.40 trials per participant) were excluded in further analysis as the experimental manipulation (coupling the direction changes of the dots with heartbeats) could not be effective. In the remaining trials, the R-peaks in real-time ECG signal were detected with high precision (hit rate: 0.99 ± 0.02 ; missing rate: 0.01 ± 0.02 ; false alarm rate: 0.02 ± 0.02).

The direction changes of the non-coupled dots were out of sync with any cardiac phase (396.87 ± 170.54 ms after R-peaks). However, there was a delay between the intended and actual timings of the "coupled" direction changes, resulting from online ECG signal processing. Diastole-coupled direction changes occurred at 120.64 ± 28.12 ms after R-peaks, and systole-coupled direction changes occurred at 405.98 ± 24.84 ms after R-peaks. While these timings may not perfectly align with the minimal and maximal points of cardiac-related physiological fluctuations, they are considered acceptable concerning the estimated strength

of the cardiac-related signals. Specifically, insights from imaging and catheter studies on cardiac function (Feher, 2012; Kolev and Zimpfer, 1995; Lewis et al., 1977; Noda et al., 2017; Sato et al., 2019) suggest that the activation of aortic and carotid baroreceptors, indicative of the strength of cardiac signals, becomes much stronger after ~ 130 ms from the R-peak, peaks between ~ 280 – 310 ms, and decreases significantly after ~ 480 ms from the R-peak. In the present study, diastole-coupled direction changes occurred when the brain had not yet received strong cardiac signals, while systole-coupled changes occurred when the brain was still exposed to strong cardiac signals. In other words, our experimental design was effectively implemented, ensuring that the direction changes associated with "systole" and "diastole" phases corresponded with periods of relatively strong and weak cardiac signals, respectively. Furthermore, similar delays have been observed in previous studies (e.g., Adelhöfer et al., 2020; Ren et al., 2022a), and comparable time periods have been employed in previous studies to distinguish phases with strong or weak cardiac signals (Garfinkel et al., 2014; Rae et al., 2020, 2018).

2.5.3. SSVEP analysis

To separately quantify the brain responses to the two groups of dots that differed in the heartbeat coupling of direction changes, we extracted SSVEPs at the stimulation frequency of each group of dots in the EEG data.

2.5.3.1. SSVEP pre-processing. The EEG data segments were first filtered using a 1 Hz high-pass filter to remove slow drifts. Subsequently, the filtered data were down-sampled to 900 Hz, which is a common multiple of both stimulation frequencies, to ensure that the data segments contained full cycles of SSVEP at integer numbers of sample points (Figueira et al., 2022). The data segment of each trial was then baseline corrected using the period ranging from -1.5 to 0 s relative to the display onset. Trials containing large artifacts were discarded (3.03 ± 5.72 trials per participant) based on a threshold of ± 200 μ V in EEG channels. The number of remaining trials per participant did not differ significantly across conditions ($F_{4,124} = 1.60$, $p = .202$, $\eta_p^2 = 0.05$). The mean, standard deviations, minimum, and maximum values for the number of trials analyzed per condition were summarized in **Supplementary Table 1**. To attenuate the influence of display onset-evoked activity on EEG spectral decomposition, the initial 1 s of stimulation was excluded for further analysis (Keitel et al., 2019; Müller et al., 2006). In addition, to exclude the influence of color change-evoked responses and potential attentional adjustment after the detection of color change, the last 5 s of stimulation was also discarded. In other words, the time of interest (TOI) for analysis was from 1 to 15 s after display onset, with a TOI of 14 s ensuring that each TOI contained full cycles of SSVEP (7.5 Hz: 105 cycles; 10 Hz: 140 cycles).

The Fourier components of the stimulus frequency (either 7.5 or 10 Hz), which represent the stimulus-locked oscillations, were extracted using the FreqTag toolbox (Figueira et al., 2022) in Matlab. Specifically, a window containing ten cycles of SSVEP (1333.33 or 1000 ms, i.e., 1200 or 900 time points, for 7.5 and 10 Hz, respectively) was shifted across each segment in steps of one cycle (133.33 or 100 ms, i.e., 120 or 90 time points), and the potential within the shifting windows was averaged in the time domain. This resulted in a single segment containing ten cycles of SSVEP, which was then transformed into the frequency domain using the Fast Fourier Transform (FFT). The sliding window approach was adopted to enhance the signal-to-noise ratio of SSVEP (Figueira et al., 2022). To avoid unexpected interaction between 7.5 Hz and 10 Hz signal, ten cycles of the stimulation frequency were contained in sliding windows, resulting in a frequency resolution of 0.75 Hz for 7.5 Hz stimuli and 1 Hz for 10 Hz stimuli.

2.5.3.2. SSVEP quantification. We analyzed both the amplitude and the phase stability of the SSVEP response at the stimulation frequency. The

SSVEP amplitude reflects the signal strength of the oscillation that is time- and phase-locked to the driving stimulus (Wieser et al., 2016), while the phase stability reflects the degree to which stimulus-evoked EEG responses are phase-locked to stimulus dynamics (Eidelman-Rothman et al., 2019; Kim et al., 2007). These two measures are highly interrelated (Moratti et al., 2007): A decrease in SSVEP amplitude primarily results from reduced phase alignment/phase stability. Many studies have found that compared with unattended stimuli, attended stimuli result in higher SSVEP amplitude (Andersen et al., 2011; Kim et al., 2007; Müller et al., 1998) as well as higher phase synchronization (Ding et al., 2006; Kashiwase et al., 2012).

Amplitude analysis. It is recommended to compare the signal-to-noise ratio (SNR) of the SSVEP amplitude rather than the raw SSVEP amplitude (Figueira et al., 2022). This is because the raw SSVEP amplitude estimate may confound SSVEP with non-SSVEP amplitude at the frequency of interest (e.g., ongoing oscillatory or non-periodic activity). To enhance the comparability between stimulation frequencies (Mora-Cortes et al., 2018; Wen et al., 2018), we computed the SNR of the SSVEP amplitude using the FreqTag toolbox (Figueira et al., 2022).

Specifically, we calculated a sliding window average in the time domain for each trial. We then combined the single-trial averaged windows into a cross-trial average for each condition prior to spectral analysis, to emphasize the portion of the oscillation that is time- and phase-locked to the driving stimulus across trials. Next, we computed the FFT of the cross-trial average. Finally, we divided the spectral amplitude at the stimulation frequency by the average amplitude of neighboring frequencies (± 1.5 or ± 2 Hz for 7.5 and 10 Hz, respectively). The resulting SNR value was then log-transformed to produce SNR in dB.

Phase stability analysis. To evaluate the temporal synchronization of the SSVEP response with the stimulus dynamics (Ji et al., 2018; Keitel et al., 2019; Kritzman et al., 2022; Wieser et al., 2016), we calculated phase stability across sliding windows for each trial, using the FreqTag toolbox (Figueira et al., 2022).

Specifically, the FFT of the signal was computed for each window in the sliding window procedure. Then, normalized complex phase values (real and imaginary part of the Fourier transform) were averaged. The absolute value (vector length) of the average was then used as the phase stability index. This function outputs a phase stability value for each electrode and trial, ranging from 0 (indicating high phase variability and thus low phase stability between windows) to 1 (indicating complete phase stability between windows). Finally, we averaged the single-trial phase stability values across trials in each condition for each participant.

2.5.4. HEP analysis

To quantify the processing of internal signals from the cardiac system while participants observed the continuous moving dots, we analyzed the HEP in the EEG data.

2.5.4.1. HEP pre-processing. The EEG data segments were first filtered using a 30 Hz low-pass filter to remove high-frequency noises. Subsequently, the EEG signal within TOI of each trial (1 – 15 s relative to display onset) was segmented into HEP epochs from -100 to 600 ms relative to the R-peak. The end point of epoch window was chosen to eliminate possible contamination by subsequent R-peaks. Furthermore, R-peaks for which the subsequent R-peak appeared within 650 ms were discarded to avoid the early components of the cardiac field artifacts of the next heartbeat (Kritzman et al., 2022; Petzschner et al., 2019).

Notably, to exclude artefactual biases from preceding heartbeats, we did not perform baseline correction on these epochs (Petzschner et al., 2019). It is highly likely that any selected time window before the R-peak, which is usually utilized for baseline correction, would be confounded by cardiac field artifacts such as those from P and Q waves preceding the R-peak. Additionally, in periods of high heart rates (small R-to-R intervals), the time window before the R-peak could also

potentially overlap with the late components of the HEP, which have been reported to persist for up to 595 ms after the R-peak (Schulz et al., 2015, 2013).

Moreover, to exclude potential confounding effects resulting from differential overlap between the direction change-evoked responses and the HEP under different conditions, we removed the direction change-evoked responses from the HEP epochs. More specifically, in Diastole condition, the HEP epochs included not only neural responses evoked by heartbeats but also those evoked by the direction change of the diastole-coupled dots, as the direction change of the diastole-coupled dots was also time-locked to the R-peak. However, in Systole condition, the direction change of the systole-coupled dots was time-locked to 290 ms after each R-peak, thus mainly contaminating the late part of the HEP. To remove these confounding responses, we extracted the direction change-evoked responses in Non-coupled condition, and then subtracted these responses from each HEP epoch in the other two conditions according to the actual interval between the R-peak and the direction change of the diastole-/systole-coupled dots (see **Supplementary Analysis** for further details). Lastly, epochs containing large artifacts were excluded based on a threshold of $\pm 100 \mu\text{V}$ in EEG channels.

The HEP in each trial was calculated by averaging across all epochs of that trial. Notably, trials in which over 50 % of HEP epochs were excluded due to high heart rates (R-to-R interval < 650 ms) or excessive noise were discarded (2.87 ± 6.63 trials per participant). This resulted in the exclusion of two participants from further HEP analysis due to an insufficient number of remaining trials (< 10 trials in one condition), leaving 30 datasets for analysis. The number of remaining trials per participant did not differ significantly across conditions ($F_{4,116} = 0.27$, $p = .833$, $\eta_p^2 = 0.01$; see **Supplementary Table 1**).

2.5.4.2. Control analysis to exclude possible effects of cardiovascular artifacts. Cardiac cycle-related EEG responses (as measured by HEP in the present study) comprise not only neural responses evoked by cardiac signals but also cardiac field artifacts and pulse-related artifacts (Kern et al., 2013). Any potential effects of cardiac cycle-related artifacts on our results should thus be carefully considered.

To ensure that the observed effect in HEP amplitude was not a result of cardiac cycle-related artifacts, we conducted two control analyses. The first involved comparing the mean ECG amplitudes within the same time window (480–540 ms after the R-peak) of the observed effect, while the second compared both the mean and variance of interbeat intervals across conditions. This approach has been recommended and utilized in recent studies (Kritzman et al., 2022; Petzschner et al., 2019).

Another approach used in prior studies to remove cardiac field artifacts is independent component analysis. However, this approach has received criticism for its limited ability to fully eliminate the cardiac field artifacts and the potential risk of removing task-related signals (Petzschner et al., 2019). For transparency, we analyzed the HEP data after applying this correction approach (see **Supplementary Analysis**). Importantly, the effects observed in the corrected HEP data were consistent with the effects observed in the uncorrected HEP data.

Additionally, we extracted the HEP amplitude during the 2.5 min resting-state condition from the same cluster and compared it with the HEP amplitude during the task (across all task trials). We found no significant difference between the two conditions, which suggests comparable cardiac processing during both the task and the resting state in the present study (see **Supplementary Analysis** for further details).

2.5.5. VEP analysis

To quantify the sensitivity to brief visual events while participants observed the continuous moving dots, we analyzed the VEP evoked by the brief color change. The EEG signal in each trial was segmented into an epoch from -100 to 600 ms relative to the onset of color change. Epochs were baseline corrected using the period from -100 to 0 ms prior to the onset of color change, and those containing large artifacts

were discarded (1.53 ± 2.27 trials per participant) based on a threshold of $\pm 100 \mu\text{V}$ in EEG channels. No participants were excluded due to insufficient number of remaining trials (> 10 trials in any condition). Furthermore, the number of remaining trials per participant did not differ significantly across conditions ($F_{4,124} = 0.63$, $p = .584$, $\eta_p^2 = 0.02$; see **Supplementary Table 1**).

2.6. Statistical analysis

2.6.1. Behavioral performance

We measured detection accuracy using the correct response rate of detecting the color change (i.e., the proportion of trials with target dots correctly identified) in Systole, Diastole, and Non-coupled conditions, separately. In addition, we calculated the sensitivity and response criteria in each condition according to signal detection theory (Green and Swets, 1966; Stanislaw and Todorov, 1999).

Specifically, in this two-choice response task where the target dots (dots that changed color) were either blue or yellow and participants needed to respond whether they were blue or yellow, we defined the hit rate as the proportion of trials with "blue" target dots correctly identified as "blue" and the false alarm rate as the proportion of trials with "yellow" target dots incorrectly identified as "blue". The sensitivity index (d') was calculated as $d' = Z(\text{Hit rate}) - Z(\text{False alarm rate})$. A higher d' value indicates a better ability to distinguish between "blue" and "yellow" target dots, reflecting higher sensitivity. The response criteria (c) was calculated as $c = -1/2[Z(\text{hit rate}) + Z(\text{false alarm rate})]$. Null false alarm rates were adjusted to $1/2 N$, where N is the number of trials with yellow target dots (Stanislaw and Todorov, 1999). A higher c value indicates a more conservative criteria, meaning participants were less likely to respond "blue" unless they were certain the target dots were blue. Conversely, a lower (or negative) c value indicates a more liberal criteria, meaning participants were more likely to respond "blue" even with less certainty.

We observed a ceiling effect in behavioral performance, i.e., most participants had the highest possible accuracy (100 %), highest possible d' values (d' values = 4.31), and no response bias (c values = 0; see **Supplementary Fig. 1**). Therefore, we performed separate nonparametric Friedman test rather than one-way repeated-measures ANOVA across the three conditions (Trial Type: Systole, Diastole, and Non-coupled) on detection accuracy, sensitivity (d') and response criteria (c), as the Friedman test does not assume normal distribution and is more robust to violations of assumptions.

2.6.2. SSVEP

In Systole condition, the direction changes of the systole-coupled dots were coupled with strong cardiac-related signals, while the non-coupled dots were coupled with on average medium-level cardiac-related signals. In Diastole condition, the direction changes of the diastole-coupled dots were coupled with weak cardiac-related signals, while the non-coupled dots were coupled with on average medium-level cardiac-related signals. To explore selective attention to the concurrently-presented dots with direction changes coupled with different strengths of cardiac-related signals, our primary aim was to compare the SSVEPs evoked by systole-coupled dots with SSVEPs evoked by non-coupled dots in Systole condition, and to compare the SSVEPs evoked by the diastole-coupled dots with SSVEPs evoked by non-coupled dots in Diastole condition. Therefore, we considered two main independent factors: Trial Type (Systole or Diastole) and Heartbeat Coupling (coupled or non-coupled).

However, given that EEG signals have varying background activities across frequencies, and that different peak amplitudes of SSVEP have been observed for the same stimuli presented at different frequencies (Srinivasan et al., 2006; Wen et al., 2018), we included Flicker Frequency (7.5 or 10 Hz) as a third independent factor. Specifically, we divided each trial type into two subtypes. In one subtype, the 7.5 Hz dots were coupled with the cardiac cycle (systole or diastole) while the 10 Hz

dots were not coupled with the cardiac cycle. In the other subtype, this was reversed. Thus, the SSVEP analysis included three independent factors: Trial Type, Heartbeat Coupling, and Flicker Frequency. Notably, we excluded the "Non-coupled" trial type from this analysis, as neither frequency was coupled with the cardiac cycle.

We used separate nonparametric cluster-based permutation analysis to determine the electrodes of interest for SSVEP amplitude and phase stability. Previous studies have consistently observed maximum amplitude and phase stability of the SSVEPs in posterior electrodes (Kastner-Dorn et al., 2018; Panitz et al., 2023), consistent with the functional localization of visual processing in the occipital area (Luck and Gaspelin, 2017). Therefore, we performed the permutation analysis over the posterior electrodes (Iz, Oz, O1, O2, POz, PO3, PO4, PO7, and PO8). As, to our best knowledge, there is no way to detect three-way interaction using permutation analysis in the FieldTrip toolbox, we performed permutation tests for all possible two-way interactions, i.e., between Trial Type and Heartbeat Coupling, between Trial Type and Flicker Frequency, as well as between Heartbeat Coupling and Flicker Frequency. We also compared systole-coupled with non-coupled dots in Systole condition, and compared diastole-coupled with non-coupled dots in Diastole condition.

Finally, the mean SSVEP amplitude and mean SSVEP phase stability per condition and participant were calculated over the cluster that revealed any significant two-way interactions or significant differences between coupled versus non-coupled dots. To confirm the effects, we performed three-way repeated-measures ANOVAs on these data and conducted planned pairwise comparisons between systole-coupled and non-coupled dots in Systole condition, as well as between diastole-coupled and non-coupled dots in Diastole condition.

2.6.3. HEP

To explore differences in HEP amplitude across the three conditions, we used a nonparametric cluster-based permutation analysis to determine the electrodes and time windows of interest for HEP. Specifically, we submitted EEG data in the time window from 300 to 600 ms relative to the R-peak and over all electrodes to a repeated-measures permutation *F*-test. This specific time window was chosen to prevent the analysis of potential cardiac field artifacts (Kritzman et al., 2022). Then, the mean HEP amplitude per condition and participant was calculated over the cluster that revealed a significant effect of Trial Type. To confirm the effects, we performed a one-way repeated-measures ANOVA (Trial Type: Systole, Diastole, and Non-coupled) on these data. Upon finding a significant effect of Trial Type, we conducted two types of post hoc analyses. First, to determine which specific conditions differed from each other, we performed pairwise comparisons with Holm correction applied for multiple comparisons. Second, to gain insight into whether the changes across conditions followed a linear progression, we conducted a linear trend analysis.

2.6.4. VEP

Similarly, to explore differences in VEP amplitude across the three conditions, we used a nonparametric cluster-based permutation analysis to determine the electrodes and time windows of interest for VEP. On the basis of earlier related research (Eiserbeck et al., 2022; Koivisto and Grassini, 2016) and inspection of the grand-averaged waveform, we submitted EEG data in the time window from 200 to 300 ms after the onset of color change and over posterior electrodes (Iz, Oz, O1, O2, POz, PO3, PO4, PO7, and PO8) to a repeated-measures permutation *F*-test. Then, the mean VEP amplitude per condition and participant was calculated over the cluster that revealed a significant effect of Trial Type. To confirm the effects, we performed a one-way repeated-measures ANOVA (Trial Type: Systole, Diastole, and Non-coupled) on these data. Upon finding a significant effect of Trial Type, we conducted both post hoc pairwise comparisons and linear trend analysis.

2.6.5. The relationship between HEP and VEP

The relationship between changes in HEP and VEP amplitude across conditions was evaluated using the Correspondence-Tradeoff Index (CTI). This index has been widely used in previous studies to quantify the trade-off or competition pattern between two brain responses (Boylan et al., 2019; Kritzman et al., 2022). Compared to correlation analysis, the CTI may be more sensitive to the trade-off between HEP and VEP amplitude in our study, given the limited number of trials available for ERP analysis.

The CTI was calculated as $CTI_{\text{between conditionA and conditionB}} = (HEP_{\text{conditionA}} - HEP_{\text{conditionB}}) * (VEP_{\text{conditionA}} - VEP_{\text{conditionB}})$. Specifically, for each participant, we calculated the difference in HEP and VEP between any two of the three conditions (Systole, Diastole, and Non-coupled), resulting in a single difference value for each measure. We then multiplied the difference value in HEP by the difference value in VEP. This procedure yielded one CTI between the Systole and Diastole conditions, one CTI between the Systole and Non-coupled conditions, and one CTI between the Diastole and Non-coupled conditions.

The CTI is negative when an increase in HEP amplitude corresponds to a decrease in VEP amplitude, and vice versa; and it is positive when both HEP and VEP amplitudes exhibit concurrent increases or decreases. To test the significance of CTI values, i.e., whether they are significantly higher or lower than zero, we conducted separate one-sample *t*-test (against zero) on the CTI values between the Systole and Diastole conditions, the CTI values between the Systole and Non-coupled conditions, and the CTI values between the Diastole and Non-coupled conditions.

All statistical analyses except permutation analyses were performed using the JASP software (version 0.19.0.0; JASP Team, 2023). Kendall's *W*, Partial eta-squared (η_p^2), and Cohen's *d* were calculated as the effect size for Friedman tests, *F*-tests, and *t*-tests, respectively. The Greenhouse-Geisser correction was applied in case of violations of the sphericity assumption. For the sake of brevity, the uncorrected degrees of freedom were reported.

Permutation analyses were performed using the FieldTrip toolbox (Oostenveld et al., 2011). This type of analysis allows for statistical tests over entire data points while still controlling for multiple comparisons (Maris and Oostenveld, 2007). More specifically, for each permutation test used in the present study, adjacent spatial or spatio-temporal points for which *t*-values exceed a threshold were clustered (dependent *t*-test; cluster-defining threshold $p = .05$; iterations = 5000). The absolute sum of the *t*-values within each cluster was defined as the cluster's weight. This weight served as the sole criterion for determining the cluster's significance. Cluster-based permutation estimates the likelihood of each cluster's weight in the actual data compared to random permutations of the dataset. The *p*-value for each cluster is defined as the proportion of random iterations that resulted in a higher cluster weight. Clusters with $p < .05$ were considered significant. For each significant cluster, we report the cluster weight, *p*-value, and the corresponding electrodes and/or time window.

3. Results

3.1. Behavioral performance

We used separate nonparametric Friedman test to compare detection accuracy, sensitivity (*d'*), and response criteria (*c*) across the three conditions (Trial Type: Systole, Diastole, and Non-coupled). The analyses did not show any significant effect of Trial Type on detection accuracy ($\chi^2(2) = 0.62, p = .734$, Kendall's *W* = 0.01), sensitivity ($\chi^2(2) = 0.53, p = .769$, Kendall's *W* = 0.01), or response criteria ($\chi^2(2) = 5.58, p = .062$, Kendall's *W* = 0.09). This is likely attributed to the ceiling effect in behavioral performance resulting from the relatively long duration of the color change (400 ms).

3.2. SSVEP measures

SSVEPs reflect the brain responses to the flickering dots. Decreased SSVEP amplitude and phase stability are generally associated with reduced visual attention (Andersen et al., 2011; Ding et al., 2006).

3.2.1. Amplitude

We used nonparametric cluster-based permutation tests to identify electrodes showing potential effects of Trial Type (Systole or Diastole), Heartbeat Coupling (coupled or non-coupled), and Flicker Frequency (7.5 or 10 Hz) on SSVEP amplitude (indexed by signal-to-noise ratio; SNR). The permutation analysis did not reveal any significant clusters for the two-way interaction between Trial Type and Flicker Frequency, nor for the two-way interaction between Heartbeat Coupling and Flicker Frequency. However, a significant cluster (electrodes: Oz and O1; $t_{\text{weight}} = -6.59$; $p = .025$) was identified for the two-way interaction between Trial Type and Heartbeat Coupling.

Based on the SSVEP amplitudes averaged over this cluster, the three-way repeated-measures ANOVA confirmed a significant interaction between Trial Type and Heartbeat Coupling (Table 1).

To further explore this interaction effect, we conducted post hoc pairwise comparisons between the two levels of Heartbeat Coupling for each Trial Type. As shown in Fig. 2, in Systole condition, systole-coupled dots triggered smaller SSVEP amplitude (19.78 ± 1.78 dB) compared to concurrently-presented non-coupled dots (20.43 ± 1.85 dB; $t_{31} = -3.19$, $p = .003$, Cohen's $d = -0.56$). In Diastole condition, diastole-coupled dots triggered marginally larger SSVEP amplitude (20.58 ± 1.79 dB) compared to concurrently-presented non-coupled dots (20.19 ± 1.90 dB; $t_{31} = 2.01$, $p = .054$, Cohen's $d = 0.36$).

The main effect of Flicker Frequency was also significant, showing that the SSVEP amplitude of 7.5 Hz visual stimuli (22.31 ± 1.90 dB) was larger than that of 10 Hz visual stimuli (18.18 ± 2.53 dB). This effect was probably due to large activation and noise in the alpha band.

3.2.2. Phase stability

Similarly, we used nonparametric cluster-based permutation tests to identify electrodes showing potential effects of Trial Type, Heartbeat Coupling, and Flicker Frequency on SSVEP phase stability. The permutation analysis did not reveal any significant clusters for the two-way interaction between Trial Type and Flicker Frequency, between Heartbeat Coupling and Flicker Frequency, or between Trial Type and Heartbeat Coupling. However, a significant cluster (electrodes: Oz, O1, and Iz; $t_{\text{weight}} = 6.43$; $p = .017$) was identified for the comparison between diastole-coupled and non-coupled dots in Diastole trials. Table 2 shows the results of the three-way repeated-measures ANOVA based on the SSVEP phase stability averaged over this cluster.

Although the two-way interaction between Trial Type and Heartbeat Coupling was not significant, to explore differences in phase stability between the concurrently-presented dots with direction changes coupled with different strengths of cardiac-related signals, we conducted planned pairwise comparisons between the two levels of Heartbeat Coupling for each Trial Type. As shown in Fig. 3, in Diastole condition, diastole-coupled dots triggered higher phase stability (0.61 ± 0.13) compared to non-coupled dots (0.59 ± 0.14 ; $t_{31} = 2.42$, $p = .022$,

Cohen's $d = 0.43$). However, in Systole condition, no significant difference in phase stability was observed between systole-coupled dots (0.60 ± 0.14) and non-coupled dots (0.59 ± 0.13 ; $t_{31} = 1.25$, $p = .220$, Cohen's $d = 0.22$).

The main effect of Heartbeat Coupling was significant, showing that the SSVEP phase stability was higher when the visual stimuli were coupled with cardiac cycle (systole or diastole; 0.60 ± 0.13), compared to when they were not coupled with cardiac cycle (0.59 ± 0.13). The main effect of Flicker Frequency was also significant, showing that the phase stability of 7.5 Hz visual stimuli (0.70 ± 0.16) was higher than that of 10 Hz visual stimuli (0.50 ± 0.14). Again, this effect was probably due to large activation and noise in the alpha band.

3.3. HEP amplitude

HEP reflects cardiac processing in the brain (Coll et al., 2021; Park et al., 2018), and larger HEP is associated with stronger attention to the cardiac system (Kritzman et al., 2022; Petzschner et al., 2019). We used a nonparametric cluster-based permutation test to identify electrodes and time windows showing potential difference in HEP amplitude across the three conditions (Trial Type: Systole, Diastole, and Non-coupled). The permutation analysis revealed a significant cluster for the effect of Trial Type on HEP amplitude (electrodes: AFz, AF4, AF7, Cz, C1, C2, C4, CP1, CP2, CP6, Fz, F1, F2, F3, F4, FCz, FC2, FC4, FP1, FT8, FT10, T8, and TP10; time window: 480–540 ms after the R-peak; $t_{\text{weight}} = 8771.24$; $p = .042$).

Based on the HEP amplitude averaged over this cluster, the one-way repeated-measures ANOVA confirmed significant difference in HEP amplitude among trial types ($F_{2,58} = 4.69$, $p = .021$, $\eta_p^2 = 0.14$; see Fig. 4). Post hoc pairwise comparisons showed significant differences between the Systole and Diastole conditions ($t_{29} = -4.45$, $p < .001$, Cohen's $d = -0.56$). That is, the HEP was larger when part of the visual stimuli (the direction change of one group of dots) were coupled with cardiac systole, compared to when part of them were coupled with cardiac diastole. However, neither the differences between the Systole and Non-coupled conditions ($t_{29} = -1.29$, $p = .320$, Cohen's $d = -0.28$) nor the differences between the Diastole and Non-coupled conditions were significant ($t_{29} = 1.44$, $p = .320$, Cohen's $d = 0.28$). That is, HEP amplitudes were comparable when part of the visual stimuli were coupled with cardiac systole or diastole, compared to when neither group of dots was coupled with heartbeats.

To further investigate the pattern observed in the repeated measures ANOVA, we conducted a linear trend analysis on HEP amplitude across the three conditions. The estimated strength of cardiac-related signals encountered by the direction changes of the dots was strongest in the Systole condition, intermediate in the Non-coupled condition, and weakest in the Diastole condition. Therefore, contrast weights were assigned as follows: Systole (1), Non-coupled (0), and Diastole (-1). This analysis revealed a linear increase in HEP amplitude (more negative) as the dots' direction changes encountered increasing strength of cardiac-related signals from the Diastole condition to the Non-coupled condition, and then to the Systole condition ($t_{29} = -4.45$, $p < .001$, Cohen's $d = -0.81$).

As recommended in recent studies (Kritzman et al., 2022; Petzschner et al., 2019), to rule out the possibility that differences in cardiac activity between conditions may have contributed to the observed effect in HEP amplitude, we conducted separate one-way repeated-measures ANOVA on the ECG amplitude averaged across the identical time window (see Supplementary Fig. 2), as well as the mean and standard deviations of interbeat intervals (see Supplementary Table 2). The analysis revealed that there were no significant differences among trial types for ECG amplitude ($F_{2,58} = 2.00$, $p = .144$, $\eta_p^2 = 0.07$), the mean of interbeat intervals ($F_{2,58} = 1.26$, $p = .287$, $\eta_p^2 = 0.04$), and the standard deviations of interbeat intervals ($F_{2,58} = 0.99$, $p = .357$, $\eta_p^2 = 0.03$). That is, the cardiovascular artifacts are constant across conditions in the present task and would not have affected the observed effects in HEP amplitude.

Table 1
ANOVA results on SSVEP amplitude.

Factor	$F_{(df=1,31)}$	p	η_p^2
Trial Type	3.00	.093	.09
Heartbeat Coupling	0.71	.407	.02
Flicker Frequency***	62.08	< .001	.67
Trial Type \times Heartbeat Coupling***	14.56	< .001	.32
Trial Type \times Flicker Frequency	0.50	.485	.02
Heartbeat Coupling \times Flicker Frequency	2.31	.139	.07
Trial Type \times Heartbeat Coupling \times Flicker Frequency	0.91	.349	.03

*** : $p < .001$.

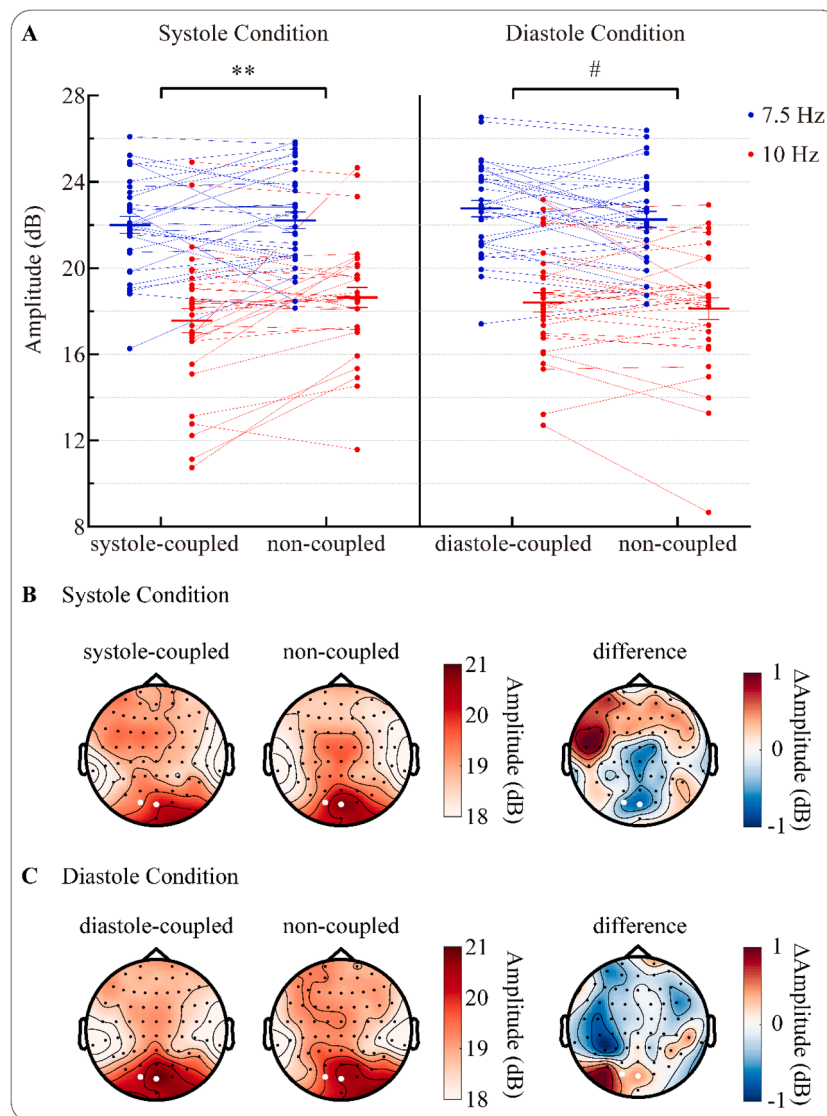


Fig. 2. SSVEP amplitude. (A) Individual (dots) and group averaged (bars) amplitude (indexed by signal-to-noise ratio; SNR) values in different conditions. The two dots corresponding to the same subject in the coupled and non-coupled conditions were connected using lines. Error bars represent standard errors. **: $p < .01$; #: marginally significant, $p < .06$. (B) Topographies of SSVEP amplitude averaged across participants for the systole-coupled and the non-coupled dots, as well as their difference in Systole condition. (C) Topographies of SSVEP amplitude averaged across participants for the diastole-coupled and the non-coupled dots, as well as their difference in Diastole condition. The electrodes used for amplitude analysis are marked in white.

Table 2
ANOVA Results on SSVEP phase stability.

Factor	$F_{(df=1,31)}$	p	η_p^2
Trial Type	0.39	.536	.01
Heartbeat Coupling**	10.64	.003	.26
Flicker Frequency***	61.60	< .001	.67
Trial Type \times Heartbeat Coupling	0.67	.420	.02
Trial Type \times Flicker Frequency	3.31	.079	.10
Heartbeat Coupling \times Flicker Frequency	1.02	.321	.03
Trial Type \times Heartbeat Coupling \times Flicker Frequency	1.05	.314	.03

** : $p < .01$.

*** : $p < .001$.

3.4. VEP amplitude evoked by the color change

The VEP reflects brain responses to the brief color change. Larger N2 component is regarded to reflect enhanced visual sensitivity (Eiserbeck et al., 2022; Koivisto and Grassini, 2016). We used a nonparametric cluster-based permutation test to identify electrodes and time windows

showing potential difference in VEP amplitude across the three trial types (Systole, Diastole, and Non-coupled). The permutation analysis revealed a significant cluster for the effect of Trial Type on the VEP amplitude (specifically, N2 component) evoked by the color change (electrodes: Iz, Oz, O1, O2, POz, PO3, PO4, and PO8; time window: 230–270 ms after the onset of the color change; $t_{weight} = 1802.11$; $p = .021$).

Based on the amplitude averaged over this cluster, the one-way repeated-measures ANOVA confirmed significant difference in N2 amplitude among trial types ($F_{2,62} = 3.71$, $p = .030$, $\eta_p^2 = 0.11$). Post hoc pairwise comparisons showed significant differences between the Systole and Diastole conditions ($t_{31} = 2.93$, $p = .019$, Cohen's $d = 0.29$; see Fig. 5). That is, the color change evoked smaller N2 when part of the visual stimuli (the direction changes of one group of dots) were coupled with cardiac systole, compared to when part of them were coupled with cardiac diastole. However, neither the differences between the Systole and Non-coupled conditions ($t_{31} = 1.09$, $p = .284$, Cohen's $d = 0.12$) nor the differences between the Diastole and Non-coupled conditions were significant ($t_{31} = -1.54$, $p = .268$, Cohen's $d = -0.17$). That is, N2

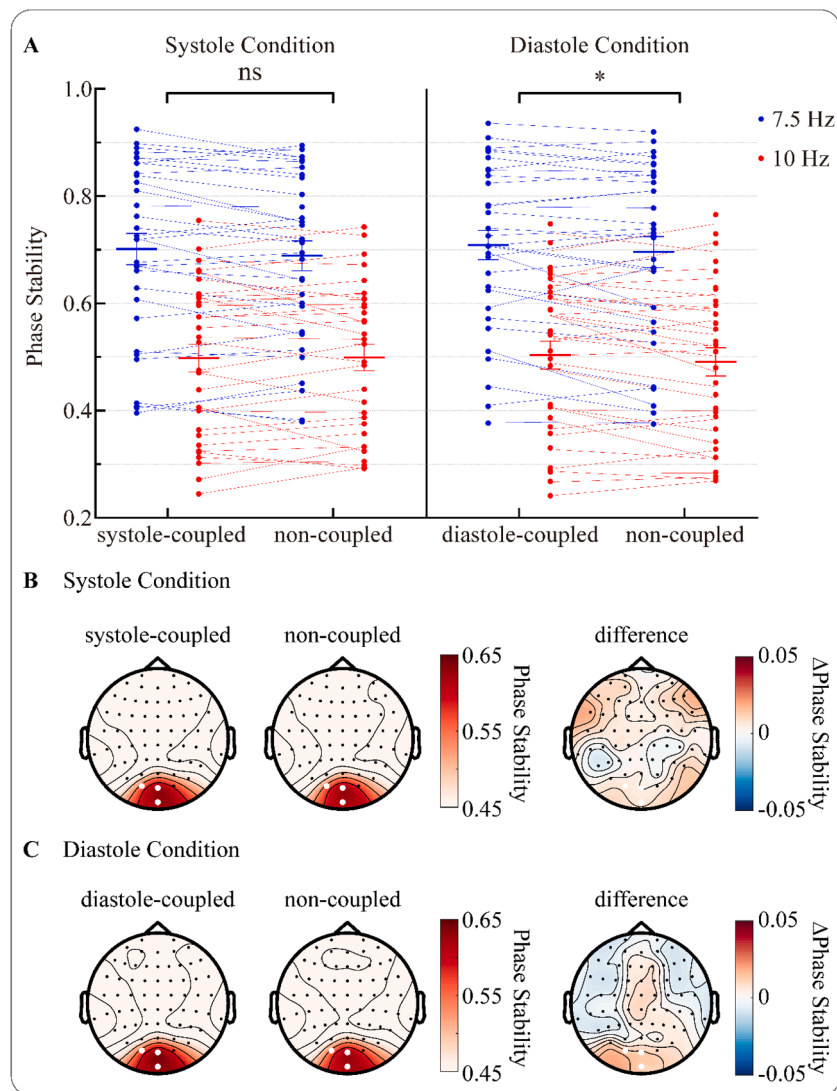


Fig. 3. SSVEP phase stability. (A) Individual (dots) and group averaged (bars) phase stability values in different conditions. The value of 1 for phase stability indicates maximum phase synchronization. The two dots corresponding to the same subject in the coupled and non-coupled conditions were connected using lines. Error bars represent standard errors. ns: not significant; *: $p < .05$. (B) Topographies of phase stability averaged across participants for the systole-coupled and the non-coupled dots, as well as their difference in Systole condition. (C) Topographies of phase stability averaged across participants for the diastole-coupled and the non-coupled dots, as well as their difference in Diastole condition. The electrodes used for phase stability analysis are marked in white.

amplitudes were comparable when part of the visual stimuli were coupled with systole or diastole, compared to when neither group of dots was coupled with heartbeats.

To further investigate the pattern observed in the repeated measures ANOVA, we conducted a linear trend analysis on VEP amplitude across the three conditions. Similar to HEP analysis, contrast weights were assigned as follows: Systole (1), Non-coupled (0), and Diastole (-1). This analysis revealed a linear decrease in N2 amplitude (less negative) as the dots' direction changes encountered increasing strength of cardiac-related signals from the Diastole condition to the Non-coupled condition, and then to the Systole condition ($t_{31} = 2.93$, $p = .006$, Cohen's $d = 0.52$).

3.5. The relationship between HEP and VEP

To explore the relationship between changes in HEP and VEP across conditions, we calculated the Correspondence-tradeoff index (CTI) according to previously established procedures (Boylan et al., 2019; Kritzman et al., 2022). The CTI is negative (significantly lower than zero) when an increase in HEP amplitude corresponds to a decrease in

VEP amplitude across conditions. Conversely, it is positive (significantly higher than zero) when both HEP and VEP amplitudes increase or decrease concurrently across conditions.

We found significantly negative CTI values between the Systole and Diastole conditions (-0.35 ± 0.92 ; $t_{29} = -2.08$, $p = .047$, Cohen's $d = -0.38$), indicating that an increase in HEP amplitude is accompanied by a decrease in VEP amplitude in Systole condition compared to Diastole condition. However, neither the CTI values between the Systole and Non-coupled conditions (0.17 ± 1.13 ; $t_{29} = 0.84$, $p = .408$, Cohen's $d = 0.15$) nor the CTI values between the Diastole and Non-coupled conditions reach significance (0.01 ± 0.97 ; $t_{29} = 0.03$, $p = .975$, Cohen's $d = 0.01$).

4. Discussion

The present study explored the spontaneous shifts of attentional and representational resources between interoception and exteroception using an EEG task where participants observed two groups of moving dots. The first group changed direction during either strong (systole-coupled), weak (diastole-coupled), or on average medium-level cardiac-

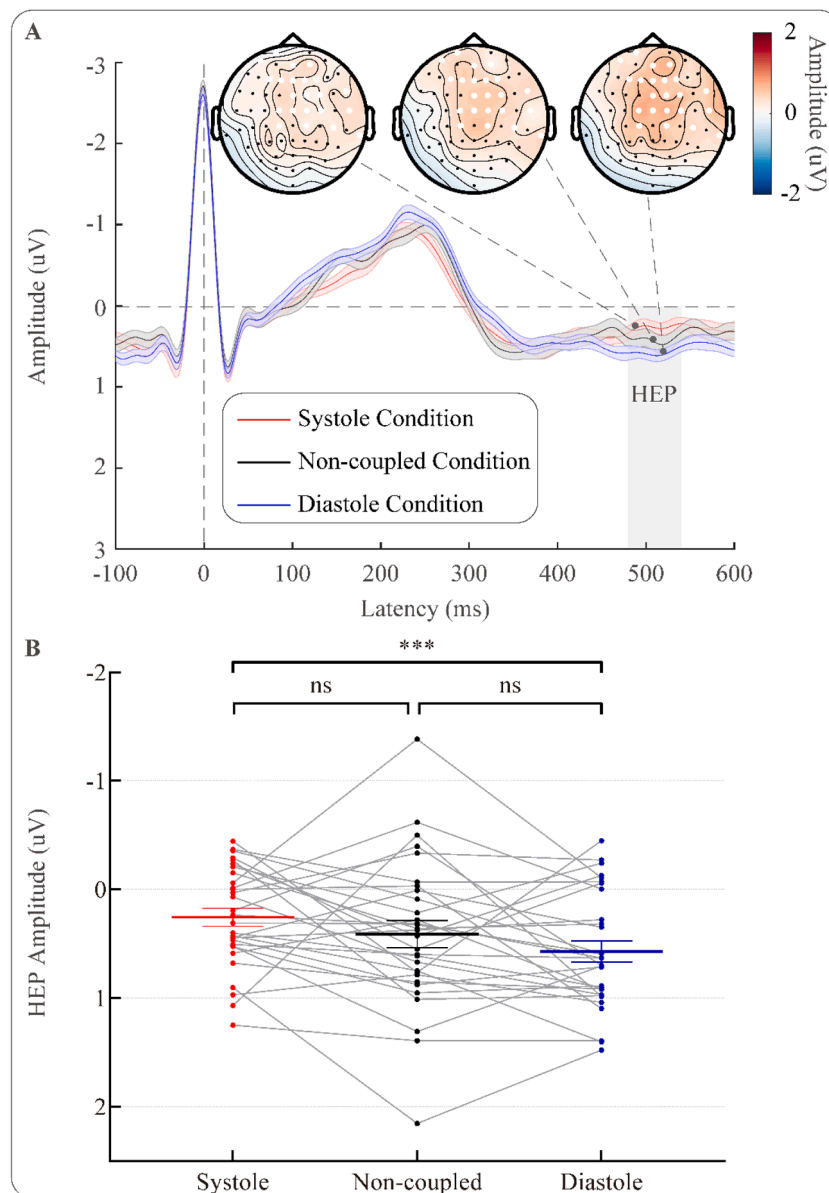


Fig. 4. Heartbeat-evoked potential (HEP). (A) Grand average HEP waveforms and topographies in different conditions. Time "0" corresponds to the time of the R-peak. The shaded bands around the lines represent standard errors. Permutation analysis revealed a significant cluster extended from 480 to 540 ms after R-peak (marked using a gray rectangle; topographies were averaged over this time window) over fronto-central electrodes (marked in white; waveforms were averaged over these electrodes). Mean HEP amplitudes were extracted from this cluster. (B) Individual (dots) and group averaged (bars) HEP amplitudes in different conditions. A larger HEP here refers to HEP with a more negative amplitude. The dots corresponding to the same subject were connected using lines. Error bars represent standard errors. ns: not significant; ***: $p < .001$.

related signals (non-coupled), compared to a second group of dots changed direction during medium-level cardiac-related signals (non-coupled). Importantly, participants' task (detecting brief color changes) did not require intentional attention to the heartbeat coupling. Using EEG frequency tagging, we independently measured the neural processing of each group of dots. We observed decreased SSVEP responses for systole-coupled dots and increased SSVEP responses for diastole-coupled dots, compared to concurrently-presented non-coupled dots. Additionally, we observed a linear increase in HEP amplitude and a linear decrease in VEP amplitude as the dots' direction changes encountered increasing strength of cardiac-related signals from the Diastole condition to the Non-coupled condition, and then to the Systole condition. Moreover, the increase in HEP amplitude across conditions was associated with the decrease in VEP amplitude. Our findings suggest not only suppressed visual processing during the cardiac phase with

stronger cardiac-related signals, but also an overall enhancement in cardiac processing and a simultaneous reduction in visual processing while the continuous visual stimuli frequently coincide with stronger cardiac-related signals. These observations support the trade-off theory between interoception and exteroception.

4.1. SSVEP results indicate reduced external attention during stronger cardiac signals

The present study directly contrasts brain responses to heartbeat-coupled and non-coupled visual stimuli that are *concurrently presented and spatially overlapping*. Previous studies typically examined the cardiac cycle effect on visual perception by comparing responses to brief events presented in different cardiac phases in separate trials (Pramme et al., 2016, 2014; Ren et al., 2022a; Walker and Sandman, 1982). However,

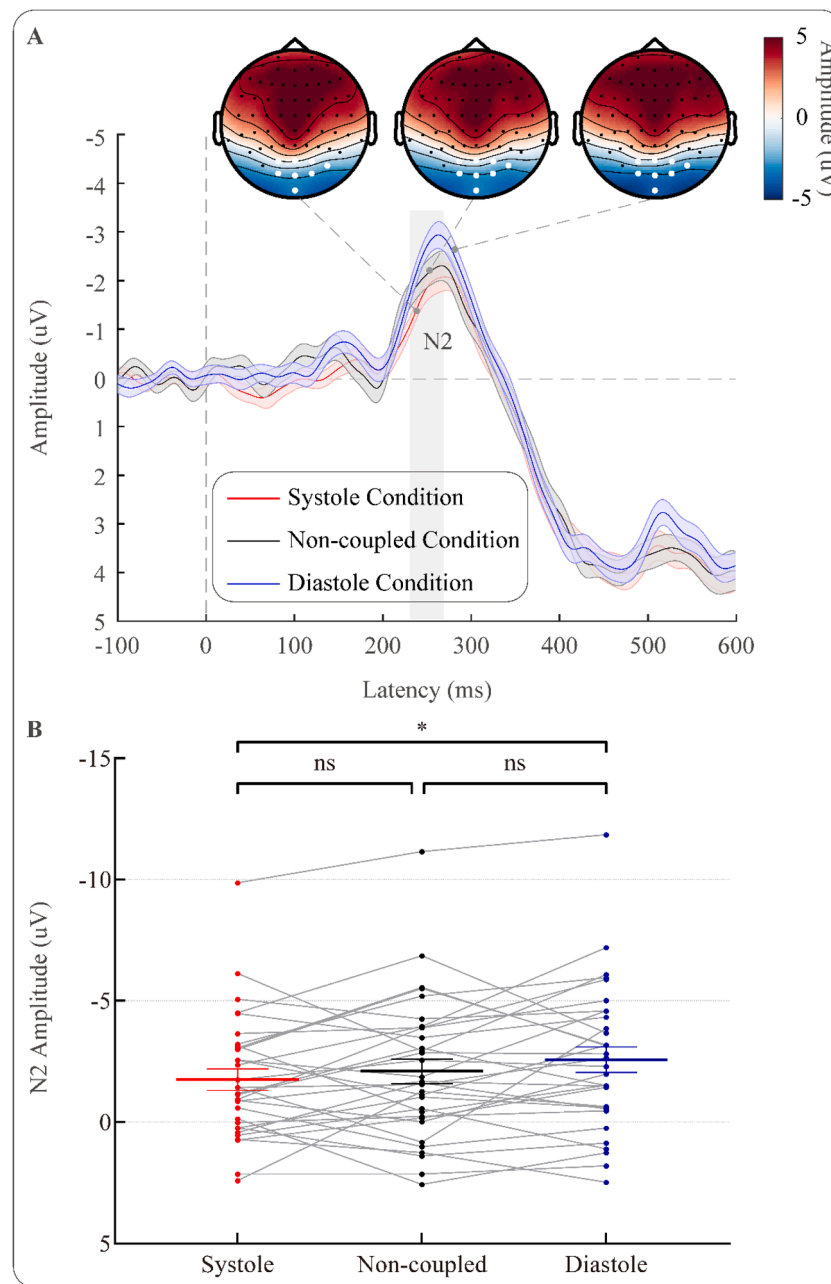


Fig. 5. N2 component evoked by the color change. (A) Grand average waveforms and topographies in different conditions. Time "0" corresponds to the onset of the color change. The shaded bands around the lines represent standard errors. Permutation analysis revealed a significant cluster extended from 230 to 270 ms after R-peak (marked using a gray rectangle; topographies were averaged over this time window) over posterior electrodes (marked in white; waveforms were averaged over these electrodes). Mean N2 amplitudes were extracted from this cluster. (B) Individual (dots) and group averaged (bars) N2 amplitudes in different conditions. A larger N2 here refers to N2 with a more negative amplitude. The dots corresponding to the same subject were connected using lines. Error bars represent standard errors. ns: not significant; *: $p < .05$.

potential confounding factors, such as differences in general brain resources or variations in spatial attention across trials, may contaminate the effects. The present study minimizes these potential confounds by presenting visual stimuli with varying heartbeat coupling simultaneously at the same spatial location.

We observed smaller SSVEP amplitude for the systole-coupled dots whose direction changes encountered strong cardiac-related signals, and larger SSVEP amplitude and phase stability for diastole-coupled dots whose direction changes encountered weak cardiac-related signals, compared to concurrently-presented non-coupled dots whose direction changes encountered on average medium-level cardiac-related signals. Decreased/increased SSVEP amplitude and phase stability are

consistently associated with reduced/increased visual attention (Andersen et al., 2011; Ding et al., 2006; Kashiwase et al., 2012; Kim et al., 2007; Morgan et al., 1996; Müller et al., 1998). Thus, our results may suggest that, while observing the two groups of moving dots, participants paid less object-based attention to the group of dots with direction changes coinciding with relatively stronger cardiac-related signals. Specifically, the brain selectively suppressed the visual representation of dots undergoing a direction change when cardiac-related signals are strong. Conversely, it appears to enhance visual information from dots that change direction when cardiac-related signals are weak. It may suggest that, during each cardiac cycle, attention towards the external world may decrease due to interference from strong

cardiac-related physiological changes, while more attention can be directed to the external environment when the interference from cardiac system is minimal. Interestingly, researchers observed that people tend to sample visual information when cardiac-related signals are weak (Galvez-Pol et al., 2020) and actively spend more time perceiving tactile stimuli during the cardiac phase with lower perceptual sensitivity (Galvez-Pol et al., 2022b). This may suggest that the brain dynamically adjusts its sampling of external stimuli based on the intrinsic changes in the allocation of brain resources along the internal-external axis in each cardiac cycle.

Furthermore, our finding indicates that the brain flexibly allocates varying degrees of processing resources to multiple visual stimuli based on their coupling with cardiac-related signals. When external sensory inputs coincide with strong internal cardiac-related signals, the brain selectively attenuates attention allocated to these specific external sensory signals rather than uniformly suppressing all external inputs.

It should be noted that, although changes in visual attention can lead to alterations in SSVEP response, it does not necessarily imply that any change in SSVEP can be solely attributed to an attentional mechanism. There are potential alternative explanations for our observations. For instance, it has been suggested that cardiac activities inhibit cortical processing (Duschek et al., 2013). This inhibition might make it look as if the brain allocates less attention to the visual stream when cardiac-related signals are stronger. However, this could be a byproduct of phasic fluctuations in cardiac physiology. In other words, a more accurate interpretation of our results may be the regulation of processing or representational resources rather than a specific attentional modulation.

Additionally, the precise mechanism behind diminished sensory processing during systole compared to diastole remains unclear. Heartbeats trigger a range of physiological alterations. Baroreceptors in the carotid sinus, coronary arteries, and aortic arch sense changes in blood pressure and send information about heartbeat strength and timing to the brainstem via the vagus nerve (Critchley and Harrison, 2013; Davos et al., 2002). Subsequently, the closed-loop arterial baroreflex system, which comprises heart rate, vascular tone, and stroke volume, buffers blood pressure variations (Vaschillo et al., 2012, 2011). Furthermore, ballistic changes in expelled blood and arterial pulsations can directly impact muscle activation (Birznieks et al., 2012; Fallon et al., 2004) and cause modest head and eye movements (Debener et al., 2010; Galvez-Pol et al., 2022a). These variations may compete for, obstruct, or interfere with the allocation of brain resources to the concurrent exteroceptive inputs (Galvez-Pol et al., 2022b). Further research is needed to determine which factors contribute to the cardiac cycle effect on the trade-off between interoception and exteroception.

The effects observed in SSVEP amplitude and phase stability are not entirely consistent. This inconsistency can be attributed to differences in the statistical sensitivities of the two measures. Specifically, SSVEP amplitude was calculated from the Fourier transform of the signal averaged across sliding windows and trials for each condition, as recommended by the SSVEP analysis toolbox (Figueira et al., 2022) for studies with a limited number of trials. In contrast, phase stability was calculated across windows within each trial and then averaged across trials for each condition. Therefore, SSVEP amplitude estimates may be less sensitive to measurement noise and other artifacts compared to phase stability measures in our study. This can lead to higher statistical sensitivity or power to detect significant differences in SSVEP amplitude than in phase stability with the same sample size. For future research, presenting systole-coupled and diastole-coupled stimuli simultaneously on the screen and directly comparing their SSVEP responses could potentially reveal stronger effects.

4.2. HEP and VEP results suggest increased internal and reduced external attention

The present study explored the changes in interoceptive cardiac

processing and exteroceptive visual processing *during the same period*. We found that HEP amplitude increased and N2 amplitude evoked by the color change decreased as the direction changes encountered increasing strength of cardiac-related signals from the Diastole condition to the Non-coupled condition, and then to the Systole condition. Larger HEP is regarded to reflect stronger internally directed attention (Petzschner et al., 2019; Villena-González et al., 2017). Thus, the HEP result may suggest increased attention to internal cardiac system while the continuous visual stimuli frequently coincided with stronger cardiac-related signals. Smaller N2 component has been regarded as reflecting reduced visual awareness (Eiserbeck et al., 2022; Koivisto and Grassini, 2016). Thus, the VEP result may suggest an overall reduced sensitivity to external visual events (e.g., color change) while the continuous visual stimuli frequently coincided with stronger cardiac-related signals.

While the null effect in behavioral performance did not align with our hypothesis, we argue that it does not weaken our interpretation of reduced visual sensitivity as indicated by the reduced VEP amplitude. The VEP response is more sensitive to the experimental manipulation than the single "blue" or "yellow" behavioral response in terms of temporal resolution. Specifically, we observed significant difference in VEP amplitude across conditions in the time window of 230–270 ms after the onset of the color change, indicating that the early visual processing of the color change was modulated by our experimental manipulation. In contrast, participants responded after observing the whole 400-ms color change, potentially leading to the ceiling effect (extremely high accuracy) observed in the behavioral data. Making the color change detection task more challenging (e.g., presenting the color change for a shorter duration) in future studies could help avoid the ceiling effect and detect potential impact of heartbeat coupling on behavioral performance.

Importantly, we found the increase in HEP amplitude across conditions corresponded to the decrease in VEP amplitude. Unlike the SSVEP results, which revealed immediate competition between cardiac-related signals and direction changes across the cardiac cycle, the trade-off pattern between increased HEP and decreased VEP reflects a longer-term effect of heartbeat coupling on the relative proportion of attentional and representational resources allocated to internal and external domain during the presentation of the continuous visual stimuli. This supports the trade-off theory between cardiac and visual processing from a new perspective. That is, the coincidence of direction changes with stronger cardiac-related signals leads to increased brain resources allocated to the internal cardiac system at the expense of reduced resources available for external visual events. One possible explanation for this phenomenon is that visual inputs occurring simultaneously with strong cardiac-related signals might be misinterpreted as signals associated with heartbeats (Al et al., 2020), thus amplifying the perceived intensity of the cardiac inputs. The resulting stronger-than-expected "cardiac signals" may lead the brain to allocate more attention to the cardiac system, as it appears to deserve more attention. This is consistent with the recent view that our brain carefully monitors internal bodily signals and is highly responsive to their changes (Tallon-Baudry, 2023). As a result, fewer brain resources are available for external information, leading to reduced sensitivity to the sudden color change.

Previous investigations primarily focused on how pre-stimulus cardiac processing affects subsequent exteroceptive processing. For instance, Park et al. (2014) found that larger pre-stimulus HEPs predicted better detection of near-threshold visual stimuli. On the contrary, Al et al. (2020) showed that larger pre-stimulus HEPs were followed by lower detection rates and electrophysiological responses for near-threshold somatosensory stimuli. Marshall et al. (2020) also showed that larger pre-stimulus HEPs predicted lower detection rates of near-threshold visual stimuli. These findings may suggest that directing more attentional and representational resources to internal heartbeats modulates the resources allocated to upcoming external events. However, whether this modulation suppresses or enhances subsequent

perception remains inconclusive. Different from these studies, the present study revealed that paying more attention to internal heartbeats reduced attention to external visual information during the same period that the continuous visual stimuli frequently coincided with strong cardiac-related signals.

4.3. Findings suggest spontaneous rather than intentional shift in internal-external processing

Prior studies instructed participants to either count visual targets (external attention condition) or their heartbeats (internal attention condition; Villena-González et al., 2017; Petzschner et al., 2019; Kritzman et al., 2022) to explore the trade-off between cardiac and visual processing. In the external attention condition, visual information was task-relevant, while cardiac information was task-irrelevant, and vice versa in the internal attention condition. They observed larger HEPs but smaller VEPs/SSVEPs in the internal attention condition compared to the external attention condition, indicating prioritization of task-relevant cardiac information over processing irrelevant visual information. Our present study diverges from their paradigms as participants were asked to detect color changes, making visual information task-relevant while cardiac activity remained irrelevant in all conditions. Thus, our findings are driven by an *automatic* process rather than a strategic regulation of brain resources or explicit judgment regarding heartbeat coupling. In other words, the SSVEP results suggest the presence of cardiac-related afferent signals automatically redirects a portion of our brain resources from the external to the internal environment. The HEP and VEP results suggest the coincidence of cardiac and visual inputs leads to a spontaneous adjustment of the relative proportion of brain resources allocated to the internal and external environment.

4.4. Variability in systole-diastole coupling: challenges in interpretation and standardization

It is worth noting that the existing literature uses various time windows to define the "systole-coupled" and "diastole-coupled" conditions, and depending on the chosen definition, this could significantly alter the interpretation of the data. Some studies define the "systole" window as the period from the ECG R-peak to the end of the T-wave (e.g., Al et al., 2020; Grund et al., 2022), others adopt a delayed "systole" window that accounts for the estimated time required for cardiac-related signals (e.g., signals from baroreceptors) to reach the brain and affect brain activities (e.g., Edwards et al., 2008; Rae et al., 2020). In the present study, stimuli were coupled to approximately 100 ms (diastole-coupled) and 400 ms (systole-coupled) after the R-peak due to an unavoidable delay resulting from real-time heartbeat coupling. We assumed that stimuli occurring at the 100 ms onset were influenced by weaker cardiac-related signals, while stimuli occurring at 400 ms onset were influenced by stronger cardiac signals. Although these timings did not perfectly align with the minimal and maximal strength of cardiac signals, they were chosen based on established physiological markers. The timing of 400 ms after the R-peak can capture the later stages of ventricular systole or the immediate effects of systolic events. This approach, although challenging due to varying heart rates and individual physiological factors, is consistent with the methodology used in many studies investigating this topic (e.g., Marshall et al., 2022; Rae et al., 2020, 2018). More importantly, our choice of timing is justified given the physiological context and the constraints of real-time heartbeat-coupling. Standardizing the definitions of systole and diastole windows based on a better understanding of cardiac-related physiological changes would improve comparability across studies in future research.

5. Conclusion

This study provides evidence for the trade-off between interoception and exteroception from two perspectives. First, in a cardiac cycle, during

cardiac phase with strong cardiac-related signals, fewer brain resources are available for external visual processing compared to cardiac phase with weak cardiac-related signals. Second, the increase in brain resources allocated to internal cardiac system caused by the co-occurrence of visual information with strong cardiac-related signals also leads to a decrease in brain resources allocated to external visual domain. Our findings highlight the dynamic, spontaneous reallocation of limited processing resources between interoception and exteroception. Furthermore, our study introduces a novel paradigm that incorporates the SSVEP frequency tagging, which holds great potential as a crucial tool for exploring the interplay between internal and external processing in both healthy individuals and those affected by interoceptive abnormalities, such as anxiety disorders, eating disorders, addictive disorders, and autism (Bonaz et al., 2021; Khalsa et al., 2018).

Funding

This work was supported by Deutsche Forschungsgemeinschaft [SCHU 24716-1 to S.S-B.] and China Scholarship Council.

CRediT authorship contribution statement

Qiaoyue Ren: Writing – original draft, Visualization, Resources, Methodology, Investigation, Formal analysis, Data curation, Conceptualization. **Amanda C. Marshall:** Writing – review & editing, Methodology. **Junhui Liu:** Writing – review & editing, Data curation. **Simone Schütz-Bosbach:** Writing – review & editing, Supervision, Methodology, Funding acquisition, Conceptualization.

Declaration of competing interest

None.

Data availability

The data generated in this study have been deposited in the OSF database under the link: https://osf.io/xkpvu/?view_only=fd28e7cea8f04b4dad5d9b0c5d7fd753.

Acknowledgments

We thank Yannick Janvier for his assistance in data collection.

Supplementary materials

Supplementary material associated with this article can be found, in the online version, at [doi:10.1016/j.neuroimage.2024.120808](https://doi.org/10.1016/j.neuroimage.2024.120808).

References

- Adelhöfer, N., Schreier, M.L., Beste, C., 2020. Cardiac cycle gated cognitive-emotional control in superior frontal cortices. *Neuroimage* 222, 117275. <https://doi.org/10.1016/j.neuroimage.2020.117275>.
- Al, E., Iliopoulos, F., Forschack, N., Nierhaus, T., Grund, M., Motyka, P., Gaebler, M., Nikulin, V.V., Villringer, A., 2020. Heart-brain interactions shape somatosensory perception and evoked potentials. *Proc. Natl. Acad. Sci.* 117, 10575–10584. <https://doi.org/10.1073/pnas.1915629117>.
- Al, E., Iliopoulos, F., Nikulin, V.V., Villringer, A., 2021. Heartbeat and somatosensory perception. *Neuroimage* 238, 118247. <https://doi.org/10.1016/j.neuroimage.2021.118247>.
- Andersen, S.K., Fuchs, S., Müller, M.M., 2011. Effects of feature-selective and spatial attention at different stages of visual processing. *J. Cogn. Neurosci.* 23, 238–246. <https://doi.org/10.1162/jocn.2009.21328>.
- Berntson, G.G., Khalsa, S.S., 2021. Neural Circuits of Interoception. *Trends Neurosci.* 44, 17–28. <https://doi.org/10.1016/j.tins.2020.09.011>.
- Birznieks, I., Boonstra, T.W., Macefield, V.G., 2012. Modulation of Human Muscle Spindle Discharge by Arterial Pulsations - Functional Effects and Consequences. *PLoS One* 7, e35091. <https://doi.org/10.1371/journal.pone.0035091>.

- Bonaz, B., Lane, R.D., Oshinsky, M.L., Kenny, P.J., Sinha, R., Mayer, E.A., Critchley, H.D., 2021. Diseases, disorders, and comorbidities of interoception. *Trends Neurosci.* 44, 39–51. <https://doi.org/10.1016/j.tins.2020.09.009>.
- Boylan, M.R., Kelly, M.N., Thigpen, N.N., Keil, A., 2019. Attention to a threat-related feature does not interfere with concurrent attentive feature selection. *Psychophysiology* 56, e13332. <https://doi.org/10.1111/psyp.13332>.
- Campbell, J.I.D., Thompson, V.A., 2012. MorePower 6.0 for ANOVA with relational confidence intervals and Bayesian analysis. *Behav. Res. Methods* 44, 1255–1265. <https://doi.org/10.3758/s13428-012-0186-0>.
- Coll, M.P., Hobson, H., Bird, G., Murphy, J., 2021. Systematic review and meta-analysis of the relationship between the heartbeat-evoked potential and interoception. *Neurosci. Biobehav. Rev.* 122, 190–200. <https://doi.org/10.1016/j.neubiorev.2020.12.012>.
- Critchley, H.D., Garfinkel, S.N., 2018. The influence of physiological signals on cognition. *Curr. Opin. Behav. Sci.* 19, 13–18. <https://doi.org/10.1016/j.cobeha.2017.08.014>.
- Critchley, H.D., Harrison, N.A., 2013. Visceral influences on brain and behavior. *Neuron* 77, 624–638. <https://doi.org/10.1016/j.neuron.2013.02.008>.
- Davos, C.H., Davies, L.C., Piepoli, M., 2002. The effect of baroreceptor activity on cardiovascular regulation. *Hellenic J. Cardiol.* 43, 145–155.
- Debener, S., Kranczioch, C., Gutberlet, I., Mulert, C., Lemieux, L., 2010. EEG quality: origin and reduction of the EEG cardiac-related artefact. EEG - fMRI: Physiological Basis, Technique, and Applications. Springer, Berlin, Heidelberg, pp. 135–151. https://doi.org/10.1007/978-3-540-87919-0_8.
- DeSaix P., Bets G.J., Johnson E., Johnson J.E., Oksana K., Kruse D.H., Poe B., Wise J.A., Young K.A., 2013. Anatomy & Physiology. OpenStax.
- Ding, J., Sperling, G., Srinivasan, R., 2006. Attentional modulation of SSVEP power depends on the network tagged by the flicker frequency. *Cereb. Cortex* 16, 1016–1029. <https://doi.org/10.1093/cercor/bhj044>.
- Duschek, S., Werner, N.S., Reyes del Paso, G.A., 2013. The behavioral impact of baroreflex function: a review: baroreflex function and behavior. *Psychophysiology* 50, 1183–1193. <https://doi.org/10.1111/psyp.12136>.
- Edwards, L., Inui, K., Ring, C., Wang, X., Kakigi, R., 2008. Pain-related evoked potentials are modulated across the cardiac cycle. *Pain* 137, 488–494. <https://doi.org/10.1016/j.pain.2007.10.010>.
- Edwards, L., Ring, C., McIntyre, D., Carroll, D., 2001. Modulation of the human nociceptive flexion reflex across the cardiac cycle. *Psychophysiology* 38, 712–718. <https://doi.org/10.1111/1469-8986.3840712>.
- Edwards, L., Ring, C., McIntyre, D., Carroll, D., Martin, U., 2007. Psychomotor speed in hypertension: effects of reaction time components, stimulus modality, and phase of the cardiac cycle. *Psychophysiology* 44, 459–468. <https://doi.org/10.1111/j.1469-8986.2007.00521.x>.
- Eidelman-Rothman, M., Ben-Simon, E., Freche, D., Keil, A., Hendler, T., Levit-Binnun, N., 2019. Sleepless and desynchronized: impaired inter trial phase coherence of steady-state potentials following sleep deprivation. *Neuroimage* 202, 116055. <https://doi.org/10.1016/j.neuroimage.2019.116055>.
- Eiserbeck, A., Enge, A., Rabovsky, M., Abdel Rahman, R., 2022. Electrophysiological chronometry of graded consciousness during the attentional blink. *Cereb. Cortex* 32, 1244–1259. <https://doi.org/10.1093/cercor/bhab289>.
- Elliott, R., Graf, V., 1972. Visual sensitivity as a function of phase of cardiac cycle. *Psychophysiology* 9, 357–361. <https://doi.org/10.1111/j.1469-8986.1972.tb03219.x>.
- Fallon, J.B., Carr, R.W., Morgan, D.L., 2004. Stochastic resonance in muscle receptors. *J. Neurophysiol.* 91, 2429–2436. <https://doi.org/10.1152/jn.00928.2003>.
- Feher, J., Feher, J., 2012. Preface. *Quantitative Human Physiology*. Academic Press, Boston, pp. ix–xi. <https://doi.org/10.1016/B978-0-12-382163-8.00098-0>.
- Figueira, J.S.B., Kutlu, E., Scott, L.S., Keil, A., 2022. The FreqTag toolbox: a principled approach to analyzing electrophysiological time series in frequency tagging paradigms. *Dev. Cogn. Neurosci.* 54, 101066. <https://doi.org/10.1016/j.dcn.2022.101066>.
- Galvez-Pol, A., Antoine, S., Li, C., Kilner, J.M., 2022a. People can identify the likely owner of heartbeats by looking at individuals' faces. *Cortex* 151, 176–187. <https://doi.org/10.1016/j.cortex.2022.03.003>.
- Galvez-Pol, A., McConnell, R., Kilner, J.M., 2020. Active sampling in visual search is coupled to the cardiac cycle. *Cognition* 196, 104149. <https://doi.org/10.1016/j.cognition.2019.104149>.
- Galvez-Pol, A., Virdee, P., Villacampa, J., Kilner, J., 2022b. Active tactile discrimination is coupled with and modulated by the cardiac cycle. *Elife* 11, e78126. <https://doi.org/10.7554/eLife.78126>.
- Garfinkel, S.N., Minati, L., Gray, M.A., Seth, A.K., Dolan, R.J., Critchley, H.D., 2014. Fear from the heart: sensitivity to fear stimuli depends on individual heartbeats. *J. Neurosci.* 34, 6573–6582. <https://doi.org/10.1523/JNEUROSCI.3507-13.2014>.
- Gjorgieva, E., Geib, B.R., Cabeza, R., Woldorff, M.G., 2022. The influence of imagery vividness and internally-directed attention on the neural mechanisms underlying the encoding of visual mental images into episodic memory. *Cereb. Cortex* bhac270. <https://doi.org/10.1093/cercor/bhac270>.
- Green, D.M., Swets, J.A., 1966. *Signal Detection Theory and Psychophysics*. Wiley, New York.
- Grund, M., Al, E., Pabst, M., Dabbagh, A., Stephani, T., Nierhaus, T., Gaebler, M., Villringer, A., 2022. Respiration, heartbeat, and conscious tactile perception. *J. Neurosci.* 42, 643–656. <https://doi.org/10.1523/JNEUROSCI.0592-21.2021>.
- JASP Team, 2023. JASP (Version 0.17.0.0)[Computer Software].
- Ji, H., Petro, N.M., Chen, B., Yuan, Z., Wang, J., Zheng, N., Keil, A., 2018. Cross multivariate correlation coefficients as screening tool for analysis of concurrent EEG-fMRI recordings. *J. Neurosci. Res.* 96, 1159–1175. <https://doi.org/10.1002/jnr.24217>.
- Kashiwase, Y., Matsumiya, K., Kuriki, I., Shioiri, S., 2012. Time courses of attentional modulation in neural amplification and synchronization measured with steady-state visual-evoked potentials. *J. Cogn. Neurosci.* 24, 1779–1793. https://doi.org/10.1162/jocn_a.00212.
- Kastner-Dorn, A.K., Andreatta, M., Pauli, P., Wieser, M.J., 2018. Hypervigilance during anxiety and selective attention during fear: using steady-state visual evoked potentials (ssVEPs) to disentangle attention mechanisms during predictable and unpredictable threat. *Cortex* 106, 120–131. <https://doi.org/10.1016/j.cortex.2018.05.008>.
- Keitel, C., Keitel, A., Benwell, C.S.Y., Daube, C., Thut, G., Gross, J., 2019. Stimulus-driven brain rhythms within the alpha band: the attentional-modulation conundrum. *J. Neurosci.* 39, 3119–3129. <https://doi.org/10.1523/JNEUROSCI.1633-18.2019>.
- Kern, M., Aertsen, A., Schulze-Bonhage, A., Ball, T., 2013. Heart cycle-related effects on event-related potentials, spectral power changes, and connectivity patterns in the human ECoG. *Neuroimage* 81, 178–190. <https://doi.org/10.1016/j.neuroimage.2013.05.042>.
- Khalsa, S.S., Adolphs, R., Cameron, O.G., Critchley, H.D., Davenport, P.W., Feinstein, J.S., Feusner, J.D., Garfinkel, S.N., Lane, R.D., Mehling, W.E., Meuret, A.E., Nemeroff, C.B., Oppenheimer, S., Petzschner, F.H., Pollatos, O., Rhudy, J.L., Schramm, L.P., Simmons, W.K., Stein, M.B., Stephan, K.E., Van den Bergh, O., Van Diest, I., von Leupoldt, A., Paulus, M.P., Ainley, V., Al Zoubi, O., Aupperle, R., Avery, J., Baxter, L., Benke, C., Berner, L., Bodurka, J., Breese, E., Brown, T., Burrows, K., Cha, Y.H., Clausen, A., Cosgrove, K., Deville, D., Duncan, L., Duquette, P., Ekhtiari, H., Fine, T., Ford, B., Garcia Cordero, I., Gleghorn, D., Guereca, Y., Harrison, N.A., Hassanpour, M., Hechler, T., Heller, A., Hellman, N., Herbert, B., Jarrahi, B., Kerr, K., Kirlic, N., Klabunde, M., Kraynak, T., Kriegsman, M., Kroll, J., Kuplicki, R., Lapidus, R., Le, T., Hagen, K.L., Mayeli, A., Morris, A., Naqvi, N., Oldroyd, K., Pané-Farré, C., Phillips, R., Poppa, T., Potter, W., Puhl, M., Safron, A., Sala, M., Savitz, J., Saxon, H., Schoenhalz, W., Stanwell-Smith, C., Teed, A., Terasawa, Y., Thompson, K., Toups, M., Umeda, S., Upshaw, V., Victor, T., Wierenga, C., Wohlrab, C., Yeh, H., Yoriss, A., Zeidan, F., Zotev, V., Zucker, N., 2018. Interoception and mental health: a roadmap. *Biol. Psychiatry Cogn. Neurosci. Neuroimaging* 3, 501–513. <https://doi.org/10.1016/j.bpsc.2017.12.004>.
- Kim, Y.J., Grabowecy, M., Paller, K.A., Muthu, K., Suzuki, S., 2007. Attention induces synchronization-based response gain in steady-state visual evoked potentials. *Nat. Neurosci.* 10, 117–125. <https://doi.org/10.1038/nn1821>.
- Koivisto, M., Grassini, S., 2016. Neural processing around 200 ms after stimulus-onset correlates with subjective visual awareness. *Neuropsychologia* 84, 235–243. <https://doi.org/10.1016/j.neuropsychologia.2016.02.024>.
- Kolev, N., Zimpfer, M., 1995. Left ventricular ejection time and end-systolic pressure revisited. *Anesth. Analg.* 81, 889.
- Kritzman, L., Eidelman-Rothman, M., Keil, A., Freche, D., Sheppes, G., Levit-Binnun, N., 2022. Steady-state visual evoked potentials differentiate between internally and externally directed attention. *Neuroimage* 254, 119133. <https://doi.org/10.1016/j.neuroimage.2022.119133>.
- Lewis, R.P., Rittgers, S.E., Froester, W.F., Boudoulas, H., 1977. A critical review of the systolic time intervals. *Circulation* 56, 146–158. <https://doi.org/10.1161/01.CIR.56.2.146>.
- Luck, S.J., Gaspelin, N., 2017. How to get statistically significant effects in any ERP experiment (and why you shouldn't). *Psychophysiology* 54, 146–157. <https://doi.org/10.1111/psyp.12639>.
- Maris, E., Oostenveld, R., 2007. Nonparametric statistical testing of EEG- and MEG-data. *J. Neurosci. Methods* 164, 177–190. <https://doi.org/10.1016/j.jneumeth.2007.03.024>.
- Marshall, A.C., Gentsch, A., Schütz-Bosbach, S., 2020. Interoceptive cardiac expectations to emotional stimuli predict visual perception. *Emotion* 20, 1113–1126. <https://doi.org/10.1037/emo0000631>.
- Marshall, A.C., Gentsch-Ebrahimzadeh, A., Schütz-Bosbach, S., 2022. From the inside out: interoceptive feedback facilitates the integration of visceral signals for efficient sensory processing. *Neuroimage* 251, 119011. <https://doi.org/10.1016/j.neuroimage.2022.119011>.
- Mora-Cortes, A., Ridderinkhof, K.R., Cohen, M.X., 2018. Evaluating the feasibility of the steady-state visual evoked potential (SSVEP) to study temporal attention. *Psychophysiology* 55, e13029. <https://doi.org/10.1111/psyp.13029>.
- Moratti, S., Clementz, B.A., Gao, Y., Ortiz, T., Keil, A., 2007. Neural mechanisms of evoked oscillations: stability and interaction with transient events. *Hum. Brain Mapp.* 28, 1318–1333. <https://doi.org/10.1002/hbm.20342>.
- Morgan, S.T., Hansen, J.C., Hillyard, S.A., 1996. Selective attention to stimulus location modulates the steady-state visual evoked potential. *Proc. Natl. Acad. Sci.* 93, 4770–4774. <https://doi.org/10.1073/pnas.93.10.4770>.
- Müller, M.M., Andersen, S., Trujillo, N.J., Valdés-Sosa, P., Malinowski, P., Hillyard, S.A., 2006. Feature-selective attention enhances color signals in early visual areas of the human brain. *Proc. Natl. Acad. Sci.* 103, 14250–14254. <https://doi.org/10.1073/pnas.0606668103>.
- Müller, M.M., Picton, T.W., Valdés-Sosa, P., Riera, J., Teder-Sälejärvi, W.A., Hillyard, S.A., 1998. Effects of spatial selective attention on the steady-state visual evoked potential in the 20–28 Hz range. *Cogn. Brain Res.* 6, 249–261. [https://doi.org/10.1016/S0926-6410\(97\)00036-0](https://doi.org/10.1016/S0926-6410(97)00036-0).
- Noda, K., Endo, H., Kadosaka, T., Nakata, T., Watanabe, T., Terui, Y., Kajitani, S., Monnma, Y., Sato, K., Kanazawa, M., Nakajima, S., Kondo, M., Takahashi, T., Nakamura, A., Nozaki, E., 2017. Comparison of the measured pre-ejection periods and left ventricular ejection times between echocardiography and impedance cardiography for optimizing cardiac resynchronization therapy. *J. Arrhythmia* 33, 130–133. <https://doi.org/10.1016/j.joa.2016.08.003>.

- Norcia, A.M., Appelbaum, L.G., Ales, J.M., Cottareau, B.R., Rossion, B., 2015. The steady-state visual evoked potential in vision research: a review. *J. Vis.* 15, 4. <https://doi.org/10.1167/15.6.4>.
- Oostenfeld, R., Fries, P., Maris, E., Schoffelen, J.M., 2011. FieldTrip: open source software for advanced analysis of MEG, EEG, and invasive electrophysiological data. *Comput. Intell. Neurosci.* 2011, 156869 <https://doi.org/10.1155/2011/156869>.
- Panitz, C., Gundlach, C., Boylan, M.R., Keil, A., Müller, M.M., 2023. Higher amplitudes in steady-state visual evoked potentials driven by square-wave versus sine-wave contrast modulation – A dual-laboratory study. *Psychophysiology* e14287. <https://doi.org/10.1111/psyp.14287>.
- Park, H.D., Bernasconi, F., Salomon, R., Tallon-Baudry, C., Spinelli, L., Seeck, M., Schaller, K., Blanke, O., 2018. Neural sources and underlying mechanisms of neural responses to heartbeats, and their role in bodily self-consciousness: an intracranial EEG study. *Cereb. Cortex* 28, 2351–2364. <https://doi.org/10.1093/cercor/bhx136>.
- Park, H.D., Correia, S., Ducorps, A., Tallon-Baudry, C., 2014. Spontaneous fluctuations in neural responses to heartbeats predict visual detection. *Nat. Neurosci.* 17, 612–618. <https://doi.org/10.1038/nn.3671>.
- Petzschner, F.H., Weber, L.A., Wellstein, K.V., Paolini, G., Do, C.T., Stephan, K.E., 2019. Focus of attention modulates the heartbeat evoked potential. *Neuroimage* 186, 595–606. <https://doi.org/10.1016/j.neuroimage.2018.11.037>.
- Pramme, L., Larra, M.F., Schächinger, H., Frings, C., 2016. Cardiac cycle time effects on selection efficiency in vision: baroreceptor activity and visual attention. *Psychophysiology* 53, 1702–1711. <https://doi.org/10.1111/psyp.12728>.
- Pramme, L., Larra, M.F., Schächinger, H., Frings, C., 2014. Cardiac cycle time effects on mask inhibition. *Biol. Psychol.* 100, 115–121. <https://doi.org/10.1016/j.biopsycho.2014.05.008>.
- Rae, C.L., Ahmad, A., Larsson, D.E.O., Silva, M., Praag, C.D.G., Garfinkel, S.N., Critchley, H.D., 2020. Impact of cardiac interoception cues and confidence on voluntary decisions to make or withhold action in an intentional inhibition task. *Sci. Rep.* 10, 4184. <https://doi.org/10.1038/s41598-020-60405-8>.
- Rae, C.L., Botan, V.E., Gould van Praag, C.D., Herman, A.M., Nyssönen, J.A.K., Watson, D.R., Duka, T., Garfinkel, S.N., Critchley, H.D., 2018. Response inhibition on the stop signal task improves during cardiac contraction. *Sci. Rep.* 8, 9136. <https://doi.org/10.1038/s41598-018-27513-y>.
- Ren, Q., Marshall, A.C., Kaiser, J., Schütz-Bosbach, S., 2022a. Multisensory integration of anticipated cardiac signals with visual targets affects their detection among multiple visual stimuli. *Neuroimage* 262, 119549. <https://doi.org/10.1016/j.neuroimage.2022.119549>.
- Ren, Q., Marshall, A.C., Kaiser, J., Schütz-Bosbach, S., 2022b. Response inhibition is disrupted by interoceptive processing at cardiac systole. *Biol. Psychol.* 170, 108323. <https://doi.org/10.1016/j.biopsycho.2022.108323>.
- Sato, K., Kumar, A., Jobanputra, Y., Betancor, J., Halane, M., George, R., Menon, V., Krishnaswamy, A., Tuzcu, E.M., Harb, S., Jaber, W.A., Mick, S., Svensson, L.G., Kapadia, S.R., 2019. Association of time between left ventricular and aortic systolic pressure peaks with severity of aortic stenosis and calcification of aortic valve. *JAMA Cardiol.* 4, 549–555. <https://doi.org/10.1001/jamacardio.2019.1180>.
- Schulz, A., Köster, S., Beutel, M.E., Schächinger, H., Vögele, C., Rost, S., Rauh, M., Michal, M., 2015. Altered patterns of heartbeat-evoked potentials in depersonalization/derealization disorder: neurophysiological evidence for impaired cortical representation of bodily signals. *Psychosom. Med.* 77, 506–516. <https://doi.org/10.1097/PSY.0000000000000195>.
- Schulz, A., Strelzyk, F., Ferreira de Sá, D.S., Naumann, E., Vögele, C., Schächinger, H., 2013. Cortisol rapidly affects amplitudes of heartbeat-evoked brain potentials—implications for the contribution of stress to an altered perception of physical sensations? *Psychoneuroendocrinology* 38, 2686–2693. <https://doi.org/10.1016/j.psyneuen.2013.06.027>.
- Srinivasan, R., Bibi, F.A., Nunez, P.L., 2006. Steady-state visual evoked potentials: distributed local sources and wave-like dynamics are sensitive to flicker frequency. *Brain Topogr.* 18, 167–187. <https://doi.org/10.1007/s10548-006-0267-4>.
- Stanislaw, H., Todorov, N., 1999. Calculation of signal detection theory measures. *Behav. Res. Methods Instrum. Comput.* 31, 137–149. <https://doi.org/10.3758/BF03207704>.
- Tallon-Baudry, C., 2023. Interoception: probing internal state is inherent to perception and cognition. *Neuron*. <https://doi.org/10.1016/j.neuron.2023.04.019>. S0896627323003045.
- Vaschillo, E.G., Vaschillo, B., Buckman, J.F., Pandina, R.J., Bates, M.E., 2012. Measurement of vascular tone and stroke volume baroreflex gain. *Psychophysiology* 49, 193–197. <https://doi.org/10.1111/j.1469-8986.2011.01305.x>.
- Vaschillo, E.G., Vaschillo, B., Pandina, R.J., Bates, M.E., 2011. Resonances in the cardiovascular system caused by rhythmical muscle tension. *Psychophysiology* 48, 927–936. <https://doi.org/10.1111/j.1469-8986.2010.01156.x>.
- Villena-González, M., Moënné-Loccoz, C., Lagos, R.A., Alliende, L.M., Billeke, P., Aboitiz, F., López, V., Cosmelli, D., 2017. Attending to the heart is associated with posterior alpha band increase and a reduction in sensitivity to concurrent visual stimuli. *Psychophysiology* 54, 1483–1497. <https://doi.org/10.1111/psyp.12894>.
- Walker, B.B., Sandman, C.A., 1982. Visual evoked potentials change as heart rate and carotid pressure change. *Psychophysiology* 19, 520–527. <https://doi.org/10.1111/j.1469-8986.1982.tb02579.x>.
- Wen, W., Brann, E., Di Costa, S., Haggard, P., 2018. Enhanced perceptual processing of self-generated motion: evidence from steady-state visual evoked potentials. *Neuroimage* 175, 438–448. <https://doi.org/10.1016/j.neuroimage.2018.04.019>.
- Wieser, M.J., Miskovic, V., Keil, A., 2016. Steady-state visual evoked potentials as a research tool in social affective neuroscience. *Psychophysiology* 53, 1763–1775. <https://doi.org/10.1111/psyp.12768>.